

Supplement of Earth Syst. Sci. Data, 12, 1897–1912, 2020
<https://doi.org/10.5194/essd-12-1897-2020-supplement>
© Author(s) 2020. This work is distributed under
the Creative Commons Attribution 4.0 License.



Open Access **Earth System
Science
Data**

Supplement of

The fate of land evaporation – a global dataset

Andreas Link et al.

Correspondence to: Andreas Link (andreas.link@tu-berlin.de)

The copyright of individual parts of the supplement might differ from the CC BY 4.0 License.

General information on the content of the supporting information (SI)

The first part of the SI provides the following supplementary figures in order to display the sample evaporationsheds of the
35 main article in monthly resolution:

- Monthly average evaporationsheds for the three chosen example land grid cells of the main article
 - Cell at 39.0° N latitude & 94.5° W longitude – Kansas City, US (Figure S1 to Figure S4)
 - Cell at 28.5° N latitude & 78.0° E longitude – Delhi, India (Figure S5 to Figure S8)
 - Cell at 0.0° latitude & 33.0° E longitude – Kampala, Uganda (Figure S9 to Figure S12)
- 40 ○ Monthly average evaporationsheds for the three chosen example countries of the main article
 - Brazil (Figure S13 to Figure S16)
 - Egypt (Figure S17 to Figure S20)
 - Laos (Figure S21 to Figure S24)
- Monthly average evaporationsheds for the three chosen example basins of the main article
 - Basin ID 1463188 – part of the Rio Grande basin (Figure S25 to Figure S28)
 - Basin ID 1019324 – part of the Danube basin (Figure S29 to Figure S32)
 - Basin ID 2245569 – part of the Murray-Darling basin (Figure S33 to Figure S36)

Based on sample scripts provided within the dataset, average monthly or yearly evaporationsheds can be plotted for any land
50 grid cell, country or basin of interest. An additional online viewer can be used to directly look up plots for any land grid cell.

The dataset and the online viewer are accessible under the following URLs:

- Dataset: <https://doi.org/10.1594/PANGAEA.908705> (Link et al., 2019a)
- Online viewer: <http://wf-tools.see.tu-berlin.de/wf-tools/evaporationshed/#/> (Link et al., 2019b)

55

Afterwards, the supplementary materials regarding chapter 4.2 of the main article are provided, which refer to the critical reflections on the used input data. They include:

- Plots regarding the average daily evaporation and precipitation based on the ERA-Interim (ERA-I) reanalysis (Berrisford et al., 2011; Dee et al., 2011) (Figure S37)
- 60 ○ Plotted differences between the ERA-I (Berrisford et al., 2011; Dee et al., 2011) and ERA5 reanalysis (Hersbach et al., 2020) regarding the average daily evaporation and precipitation (Figure S38)
- Methodological details regarding the continental comparison of the average evaporation and precipitation between ERA-I (Berrisford et al., 2011; Dee et al., 2011), ERA5 (Hersbach et al., 2020) and the study by Rodell et al. (2015)
- Grouping procedure for the aggregation of the ERA-I (Berrisford et al., 2011; Dee et al., 2011) and ERA5 data (Hersbach et al., 2020) on evaporation and precipitation to continental scales (Table S1)

The last part of the SI is given in table format and is related to chapter 4.3 of the main article (“Comparison to other datasets”).

It provides the following materials:

- Overall comparison between the country results of the 3D quasi-isentropic back-trajectory (3D QIBT) method by
70 Dirmeyer et al. (2009) and the WAM-2layers model (Van der Ent, 2014) (Table S2)
 - In this context, all comparable values for the terrestrial evaporative source (TES – unit: %) as well as the country internal evaporative source (CIES – unit: %) of precipitation are listed
- Top 10 sources of precipitation for the sample countries Brazil, Egypt and Laos – Comparison between results of the 3D QIBT (Dirmeyer et al., 2009) and the WAM-2layers model (Van der Ent, 2014) (Table S3 to Table S5)

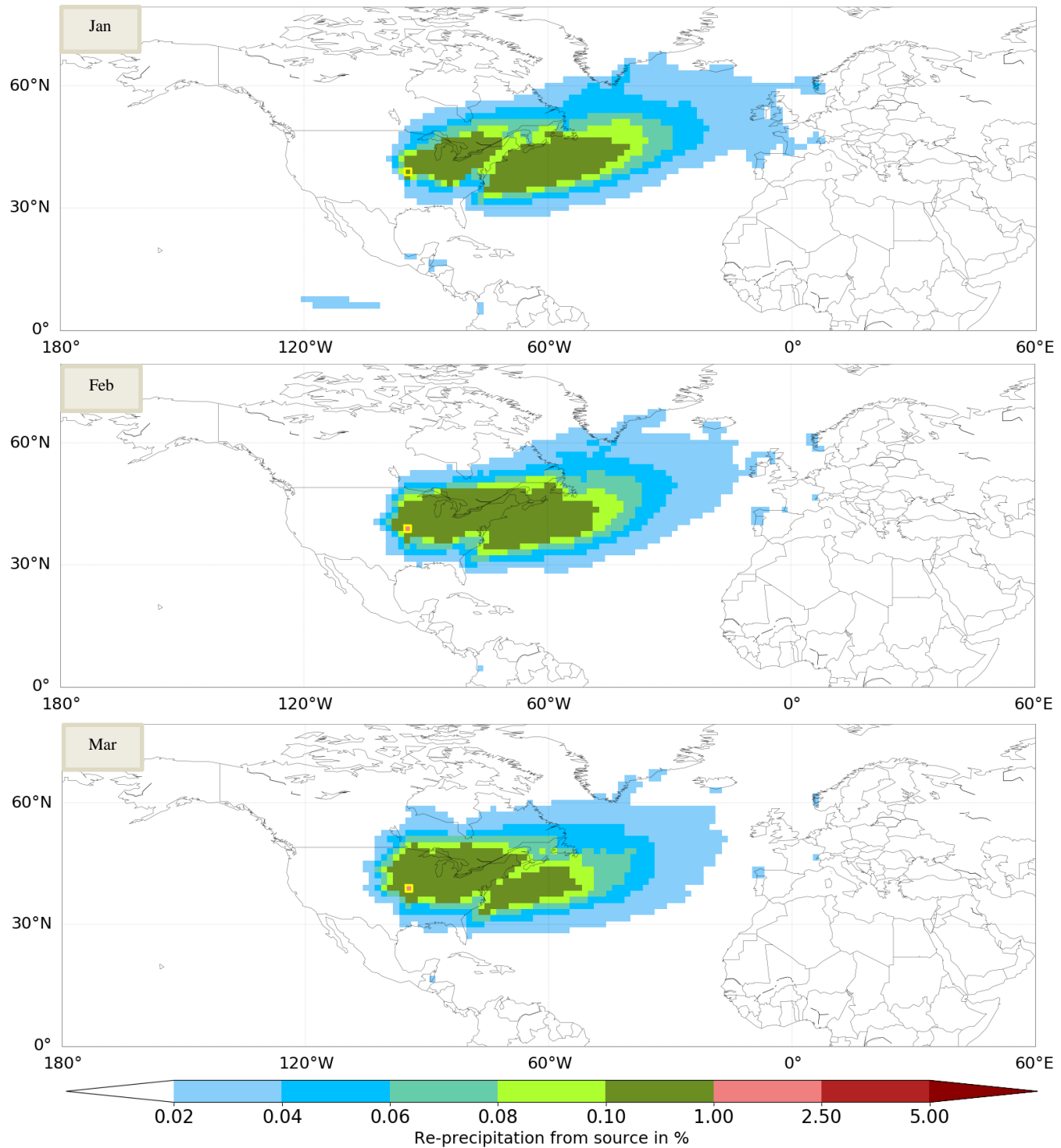


Figure S1 Monthly evaporation sheds (Jan = January, Feb = February, Mar = March) for the grid cell at 39.0° N latitude & 94.5° W longitude (Kansas City, US), E_{input} : 16.2 mm/month (Jan) / 23.1 mm/month (Feb) / 50.8 mm/month (Mar), Unassigned : 1.2 % (Jan) / 1.1 % (Feb) / 0.9 % (Mar), Colored area covers 73.8 % (Jan) / 75.5 % (Feb) / 75.4 % (Mar) of the assigned water

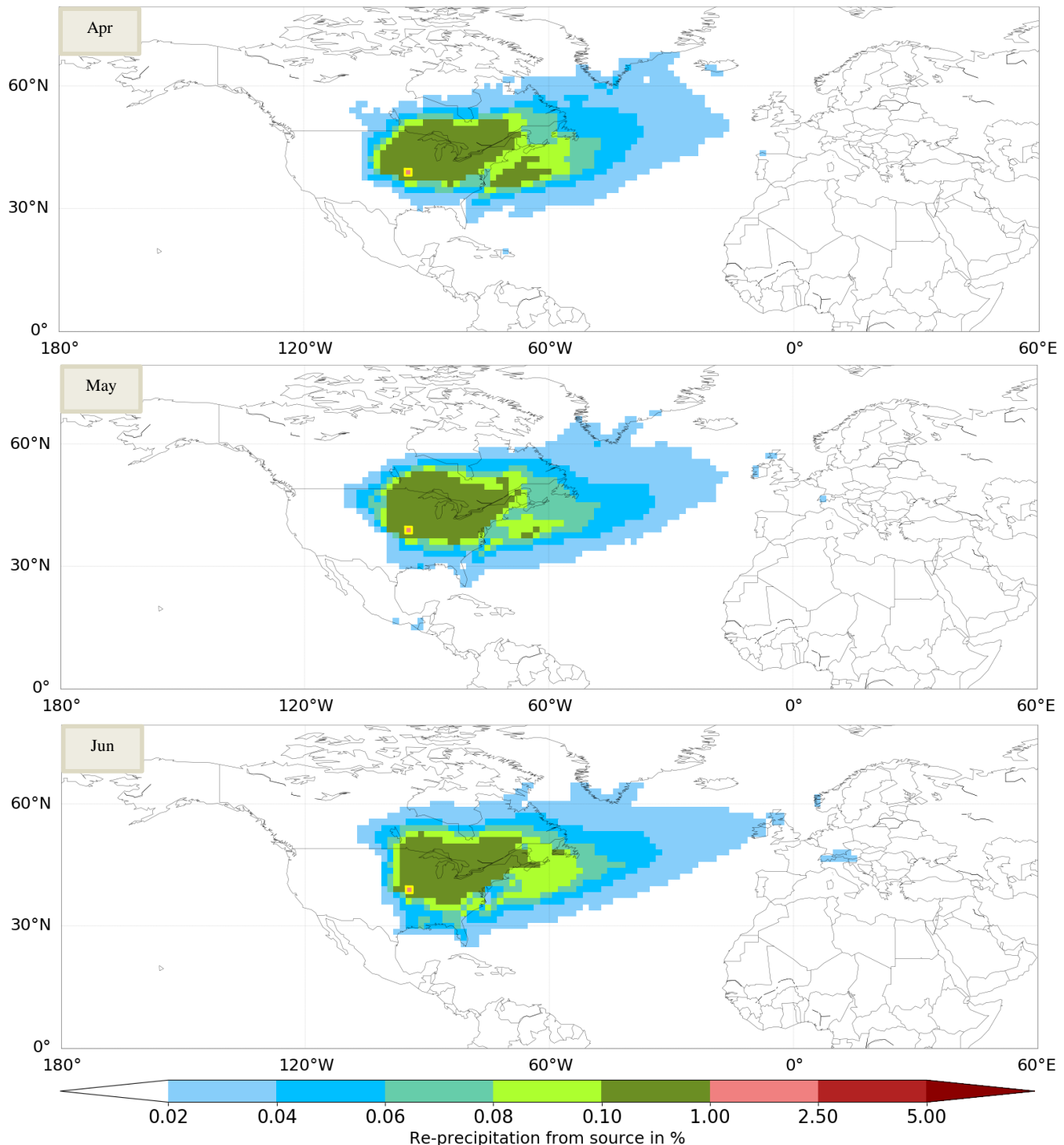


Figure S2 Monthly evaporation sheds (Apr = April, May, Jun = June) for the grid cell at 39.0° N latitude & 94.5° W longitude (Kansas City, US), E_{input} : 76.7 mm/month (Apr) / 113.0 mm/month (May) / 137.9 mm/month (Jun), Unassigned : 1.3 % (Apr) / 1.6 % (May) / 2.5 % (Jun), Colored area covers 73.9 % (Apr) / 73.9 % (May) / 74.4 % (Jun) of the assigned water

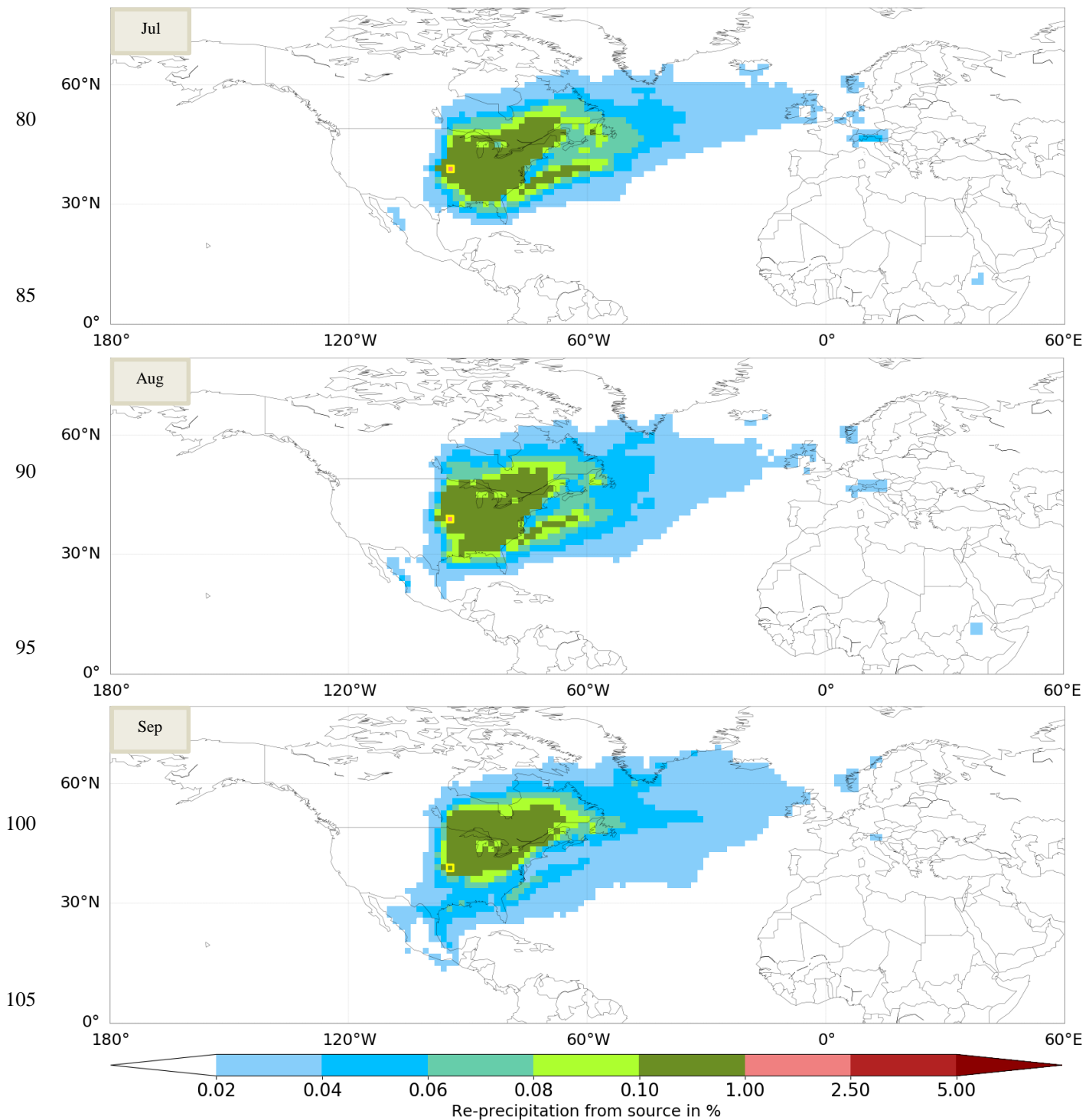


Figure S3 Monthly evaporationsheds (Jul = July, Aug = August, Sep = September) for the grid cell at 39.0° N latitude & 94.5° W longitude (Kansas City, US), E_{input} : 144.0 mm/month (Jul) / 121.6 mm/month (Aug) / 87.1 mm/month (Sep), Unassigned : 3.4 % (Jul) / 2.6 % (Aug) / 3.0 % (Sep), Colored area covers 71.0 % (Jul) / 68.9 % (Aug) / 68.9 % (Sep) of the assigned water

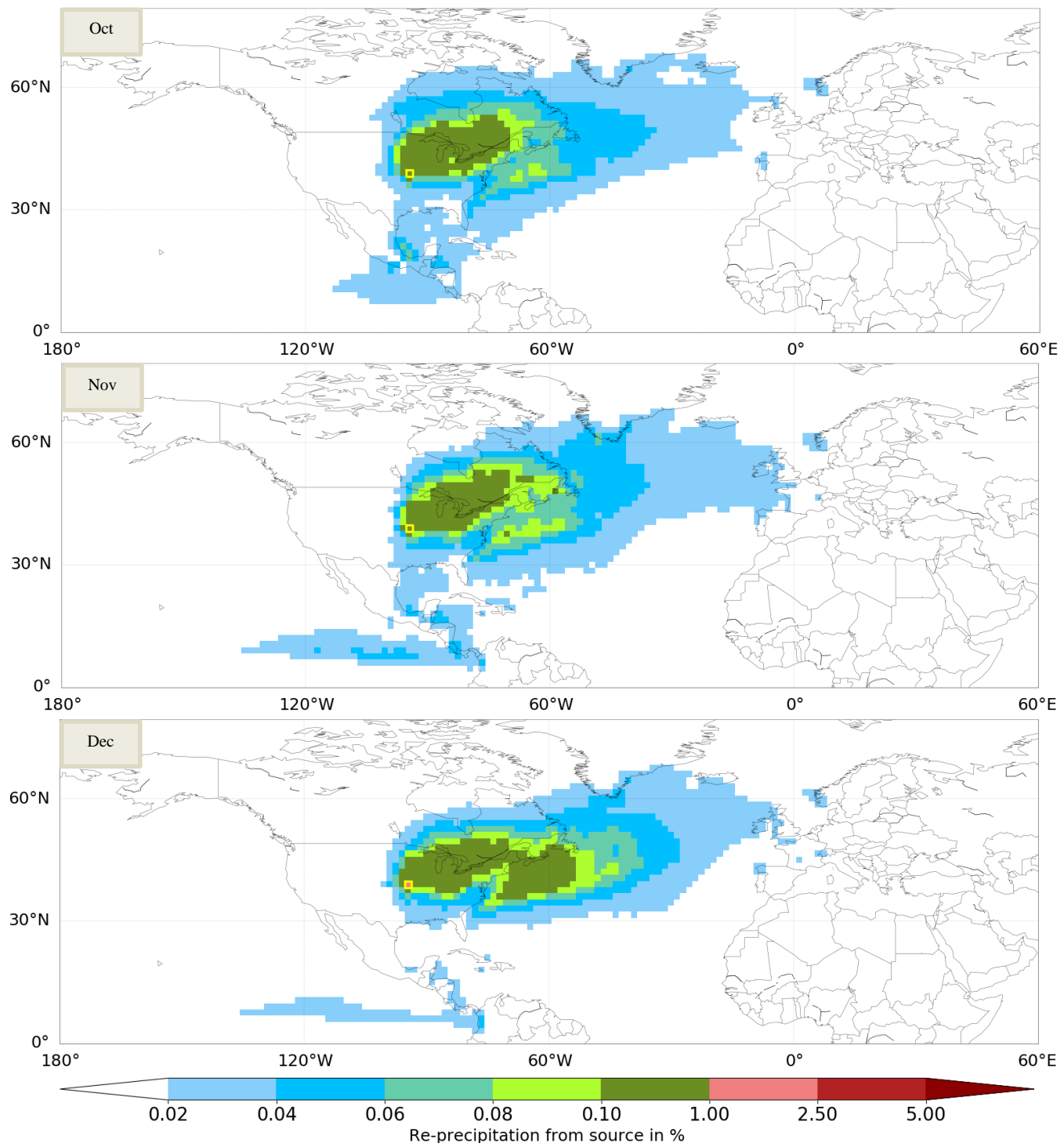


Figure S4 Monthly evaporation sheds (Oct = October, Nov = November, Dec = December) for the grid cell at 39.0° N latitude & 94.5° W longitude (Kansas City, US), E_{input} : 54.3 mm/month (Oct) / 30.1 mm/month (Nov) / 16.8 mm/month (Dec), Unassigned : 2.6 % (Oct) / 1.5 % (Nov) / 1.2 % (Dec), Colored area covers 68.3 % (Oct) / 71.1 % (Nov) / 71.1 % (Dec) of the assigned water

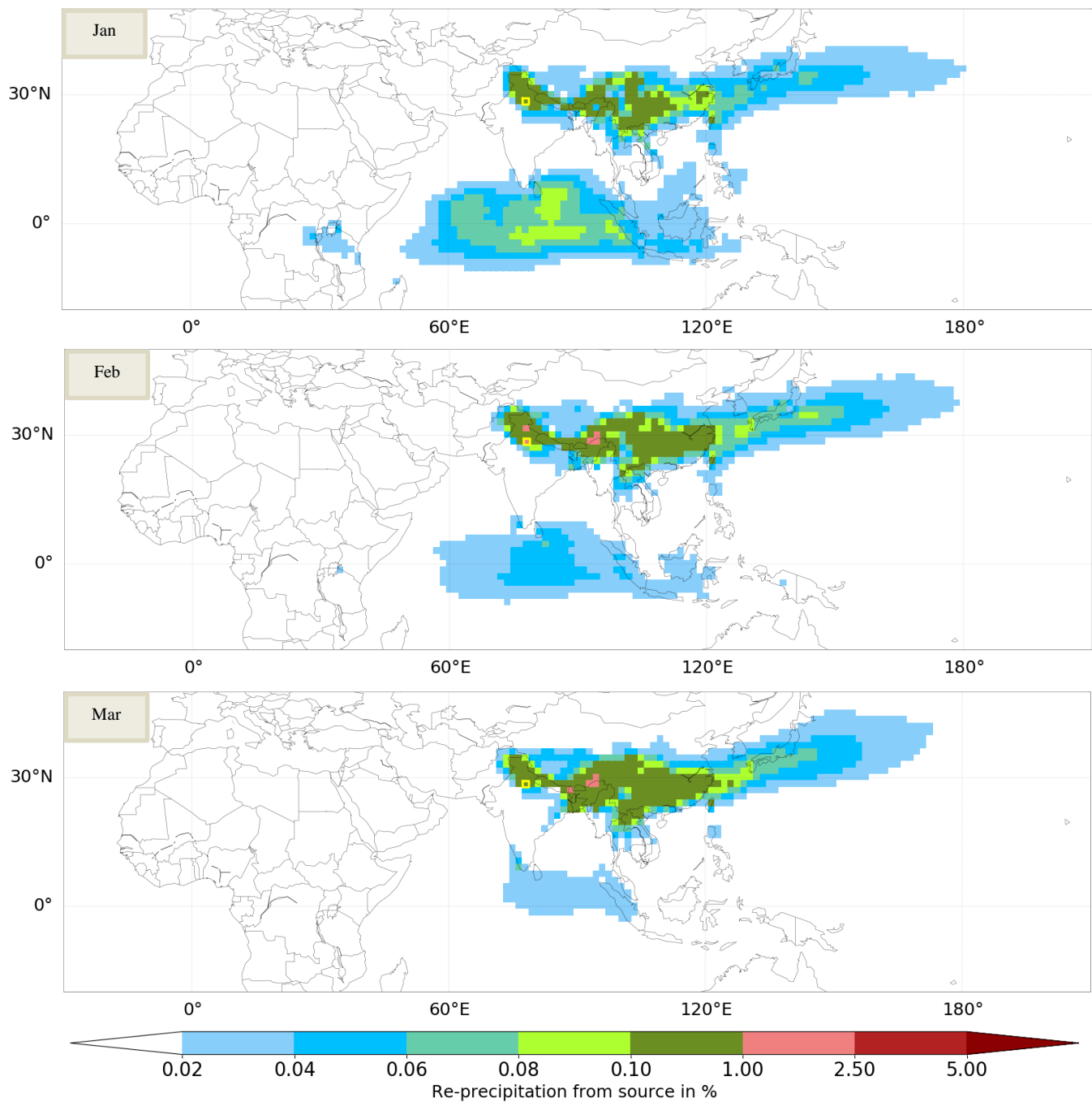


Figure S5 Monthly evaporationsheds (Jan = January, Feb = February, Mar = March) for the grid cell at 28.5° N latitude & 78.0° E longitude (Delhi, India), E_{input} : 52.3 mm/month (Jan) / 67.7 mm/month (Feb) / 98.1 mm/month (Mar), Unassigned : 0.1 % (Jan) / 0.1 % (Feb) / 0.2 % (Mar), Colored area covers 72.2 % (Jan) / 72.9 % (Feb) / 75.0 % (Mar) of the assigned water

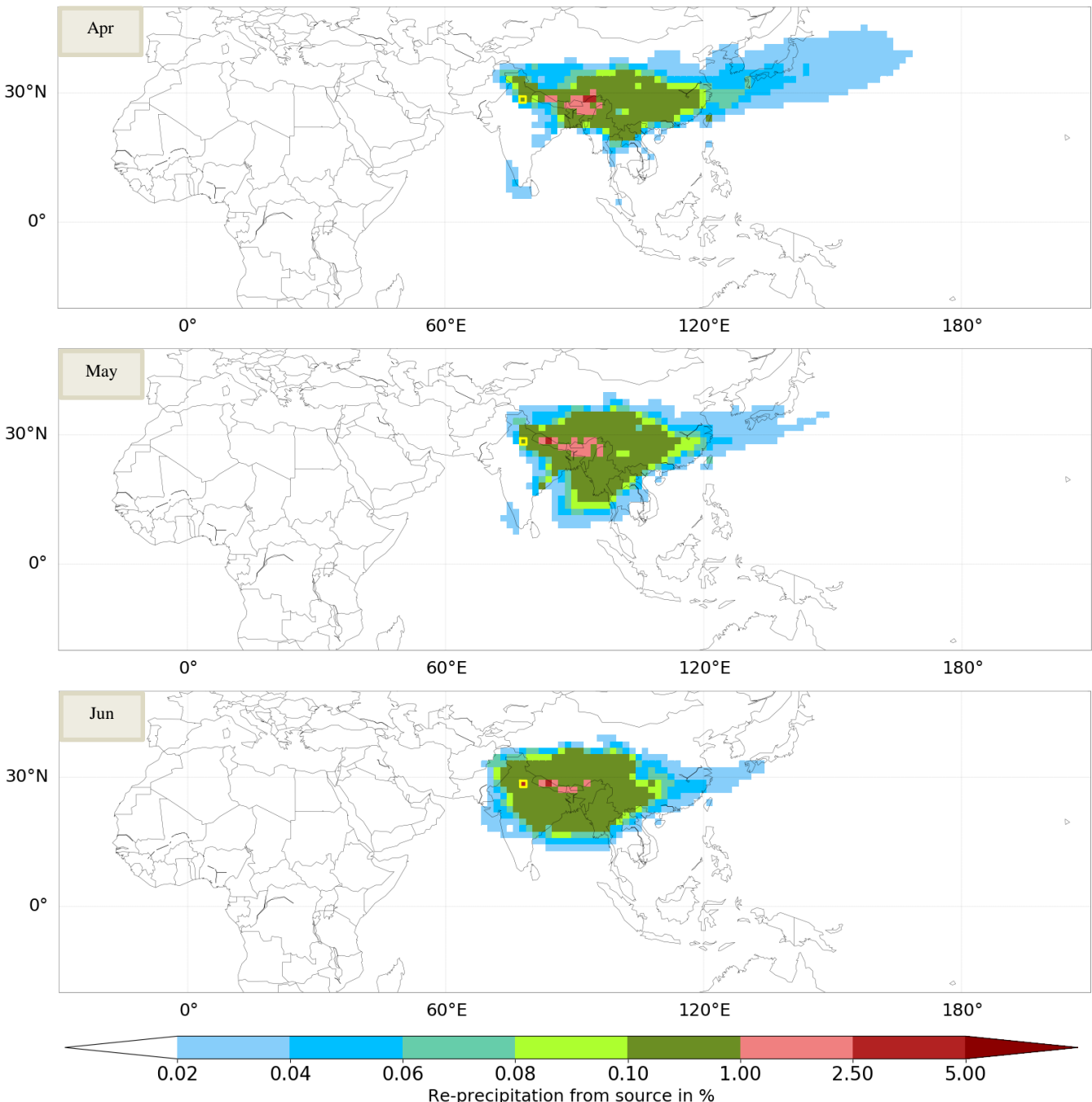


Figure S6 Monthly evaporation sheds (Apr = April, May, Jun = June) for the grid cell at 28.5° N latitude & 78.0° E longitude (Delhi, India), E_{input} : 96.4 mm/month (Apr) / 110.5 mm/month (May) / 113.8 mm/month (Jun), Unassigned : 0.2 % (Apr) / 0.3 % (May) / 0.2 % (Jun), Colored area covers 79.4 % (Apr) / 84.4 % (May) / 89.0 % (Jun) of the assigned water

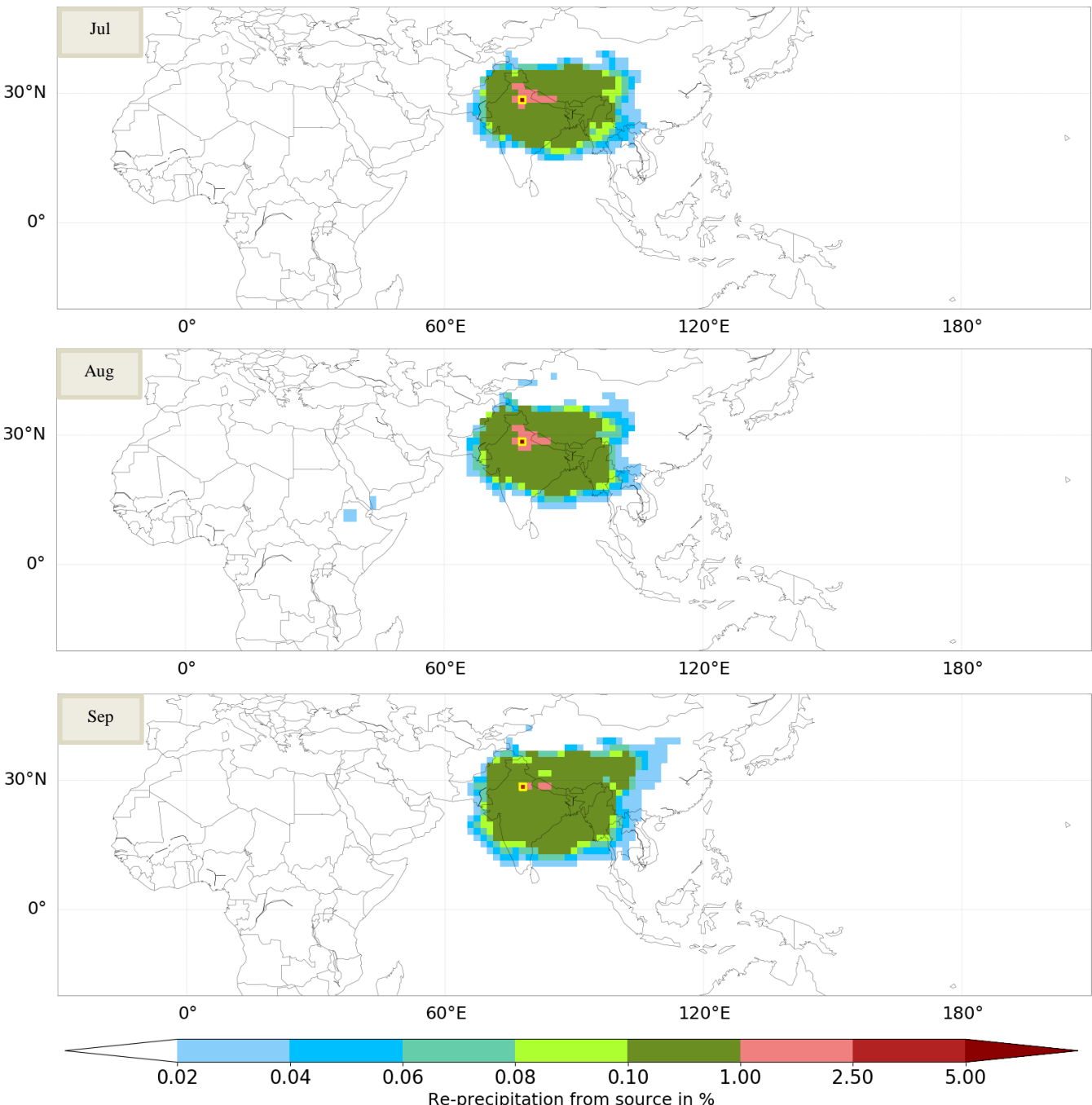


Figure S7 Monthly evaporationsheds (Jul = July, Aug = August, Sep = September) for the grid cell at 28.5° N latitude & 78.0° E longitude (Delhi, India), E_{input} : 130.4 mm/month (Jul) / 130.6 mm/month (Aug) / 123.4 mm/month (Sep), Unassigned : 0.2 % (Jul) / 0.1 % (Aug) / 0.1 % (Sep), Colored area covers 93.4 % (Jul) / 93.8 % (Aug) / 91.9 % (Sep) of the assigned water

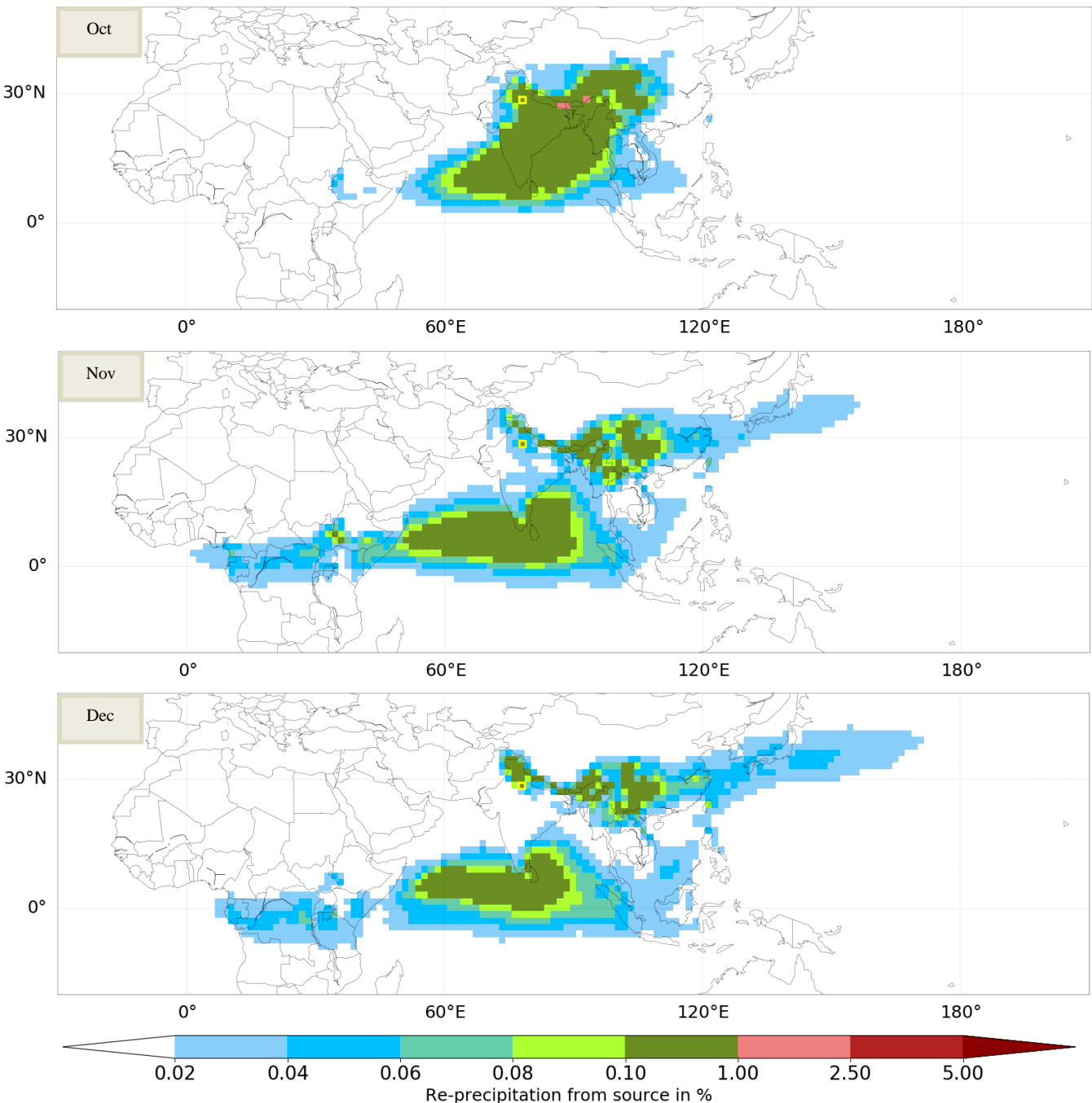


Figure S8 Monthly evaporation sheds (Oct = October, Nov = November, Dec = December) for the grid cell at 28.5° N latitude & 78.0° E longitude (Delhi, India), E_{input} : 101.2 mm/month (Oct) / 62.1 mm/month (Nov) / 46.2 mm/month (Dec), Unassigned : 0.1 % (Oct) / 0.1 % (Nov) / 0.1 % (Dec), Colored area covers 85.3 % (Oct) / 78.5 % (Nov) / 74.1 % (Dec) of the assigned water

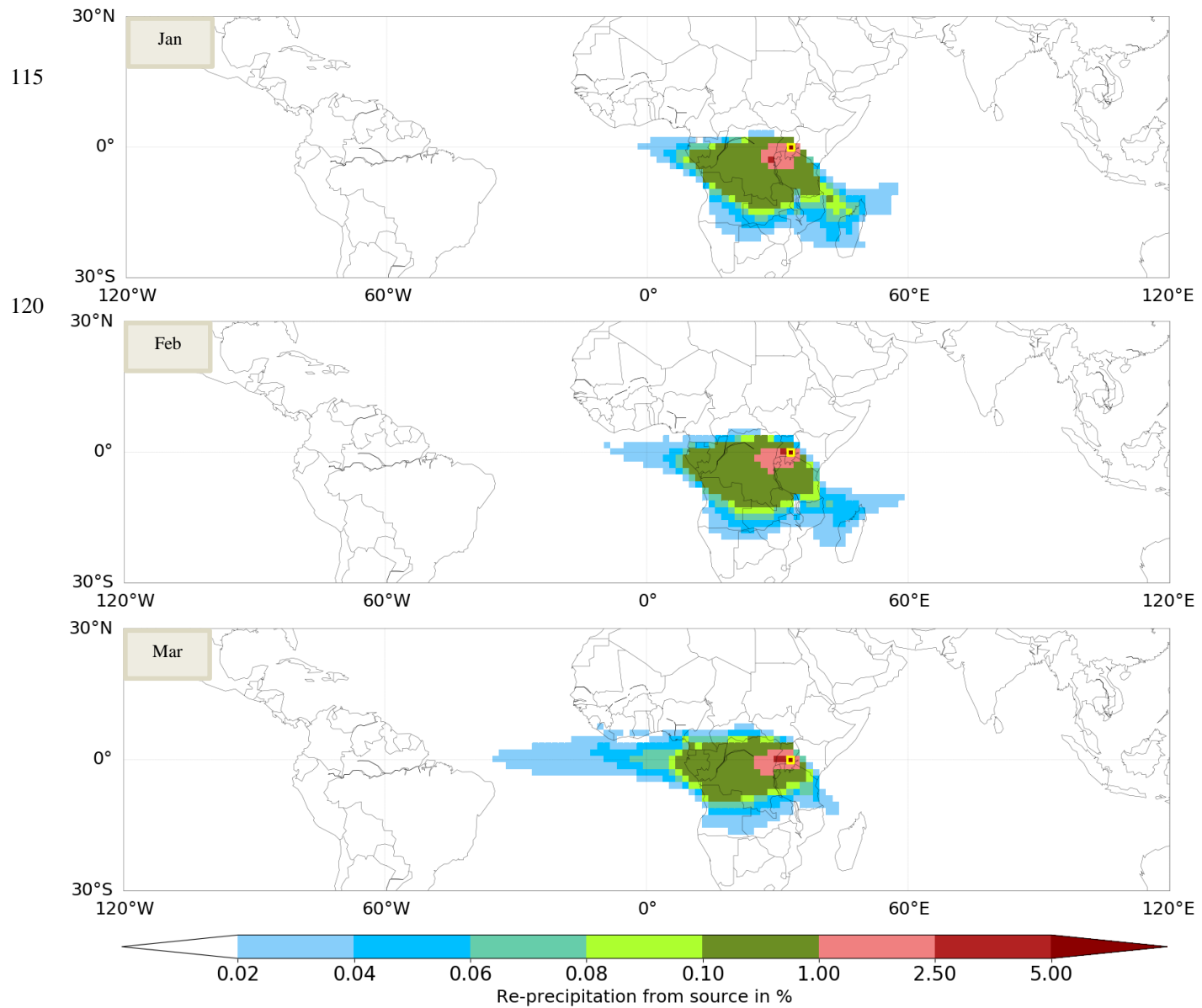


Figure S9 Monthly evaporation sheds (Jan = January, Feb = February, Mar = March) for the grid cell at 0.0° latitude & 33.0° E longitude (Kampala, Uganda), E_{input} : 104.5 mm/month (Jan) / 103.5 mm/month (Feb) / 108.9 mm/month (Mar), Unassigned : 0.0 % (Jan) / 0.0 % (Feb) / 0.0 % (Mar), Colored area covers 92.1 % (Jan) / 92.0 % (Feb) / 92.6 % (Mar) of the assigned water

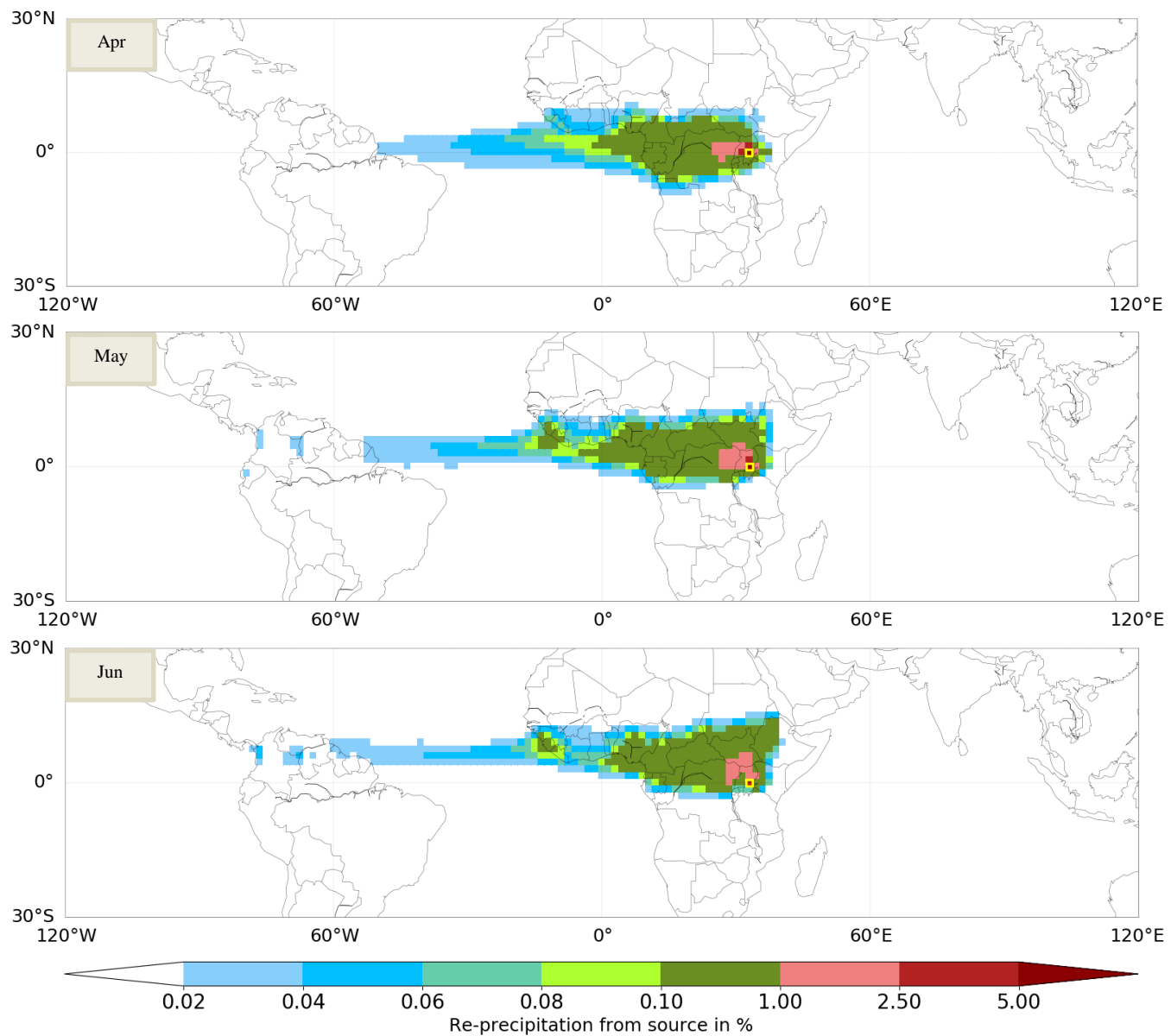


Figure S10 Monthly evaporation sheds (Apr = April, May, Jun = June) for the grid cell at 0.0° latitude & 33.0° E longitude (Kampala, Uganda), E_{input} : 93.3 mm/month (Apr) / 92.8 mm/month (May) / 86.8 mm/month (Jun), Unassigned : 0.0 % (Apr) / 0.0 % (May) / 0.0 % (Jun), Colored area covers 93.8 % (Apr) / 92.1 % (May) / 89.4 % (Jun) of the assigned water

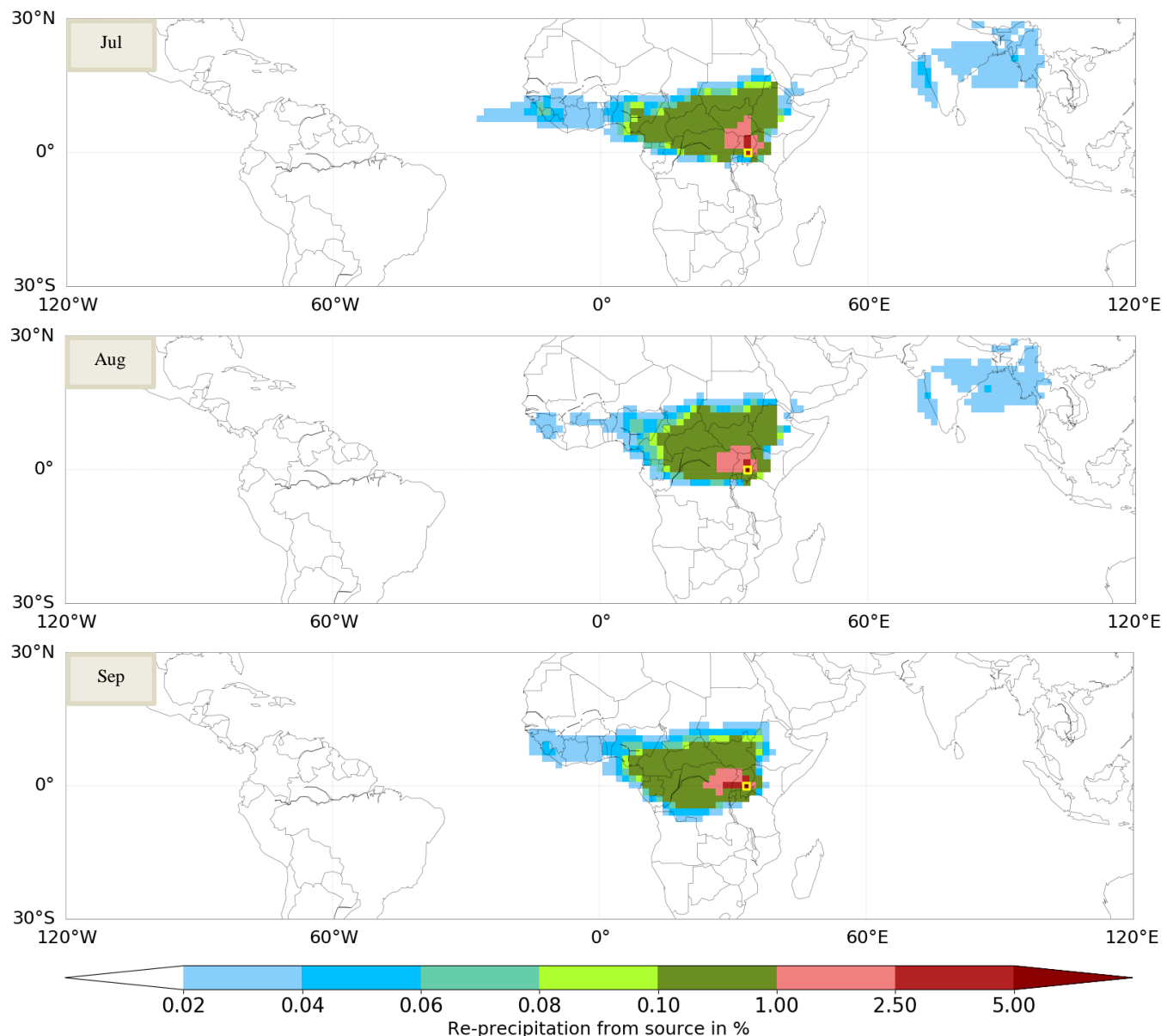


Figure S11 Monthly evaporation sheds (Jul = July, Aug = August, Sep = September) for the grid cell at 0.0° latitude & 33.0° E longitude (Kampala, Uganda), E_{input} : 87.7 mm/month (Jul) / 88.0 mm/month (Aug) / 93.9 mm/month (Sep), Unassigned : 0.0 % (Jul) / 0.0 % (Aug) / 0.0 % (Sep), Colored area covers 88.6 % (Jul) / 89.3 % (Aug) / 92.6 % (Sep) of the assigned water

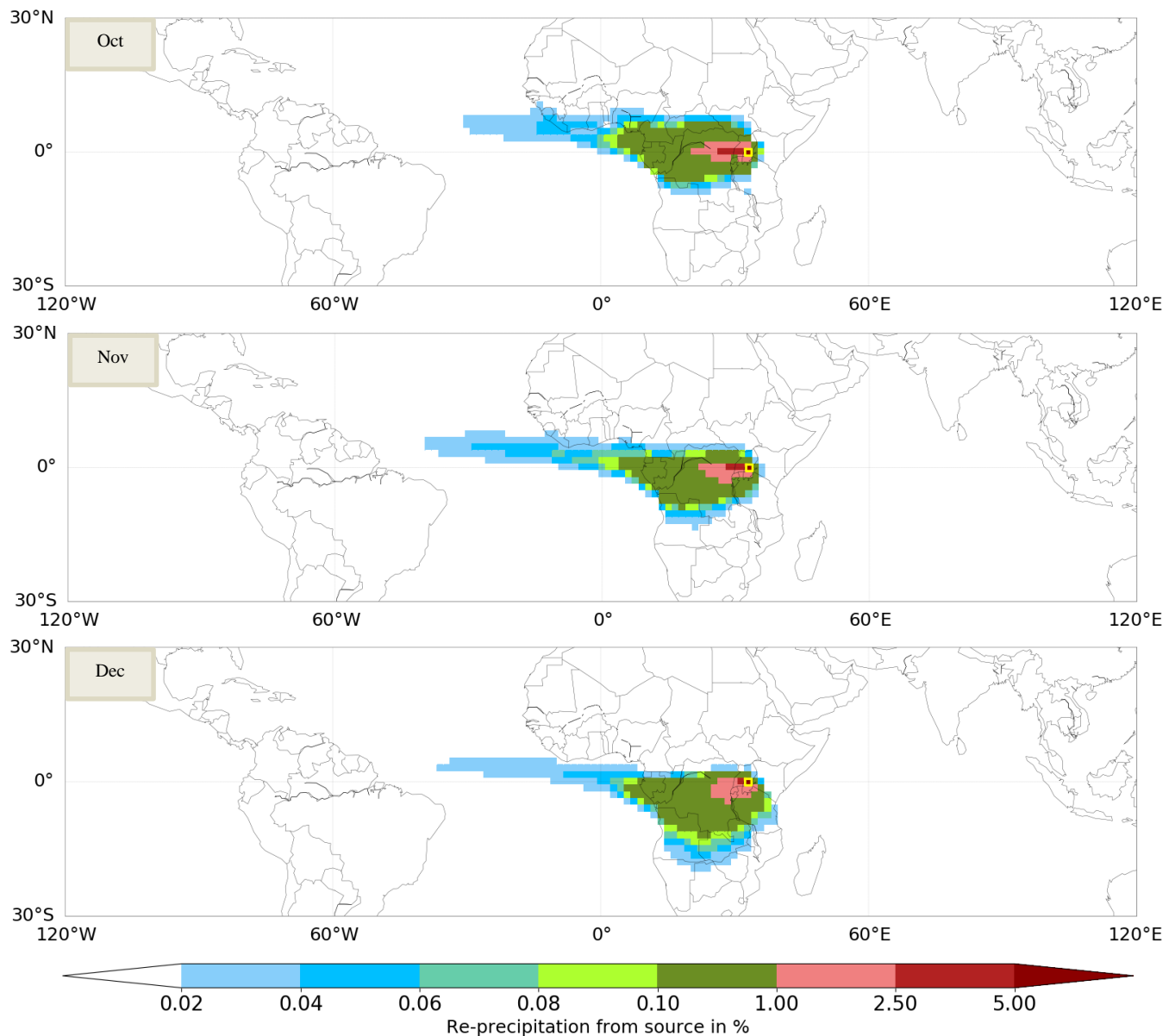
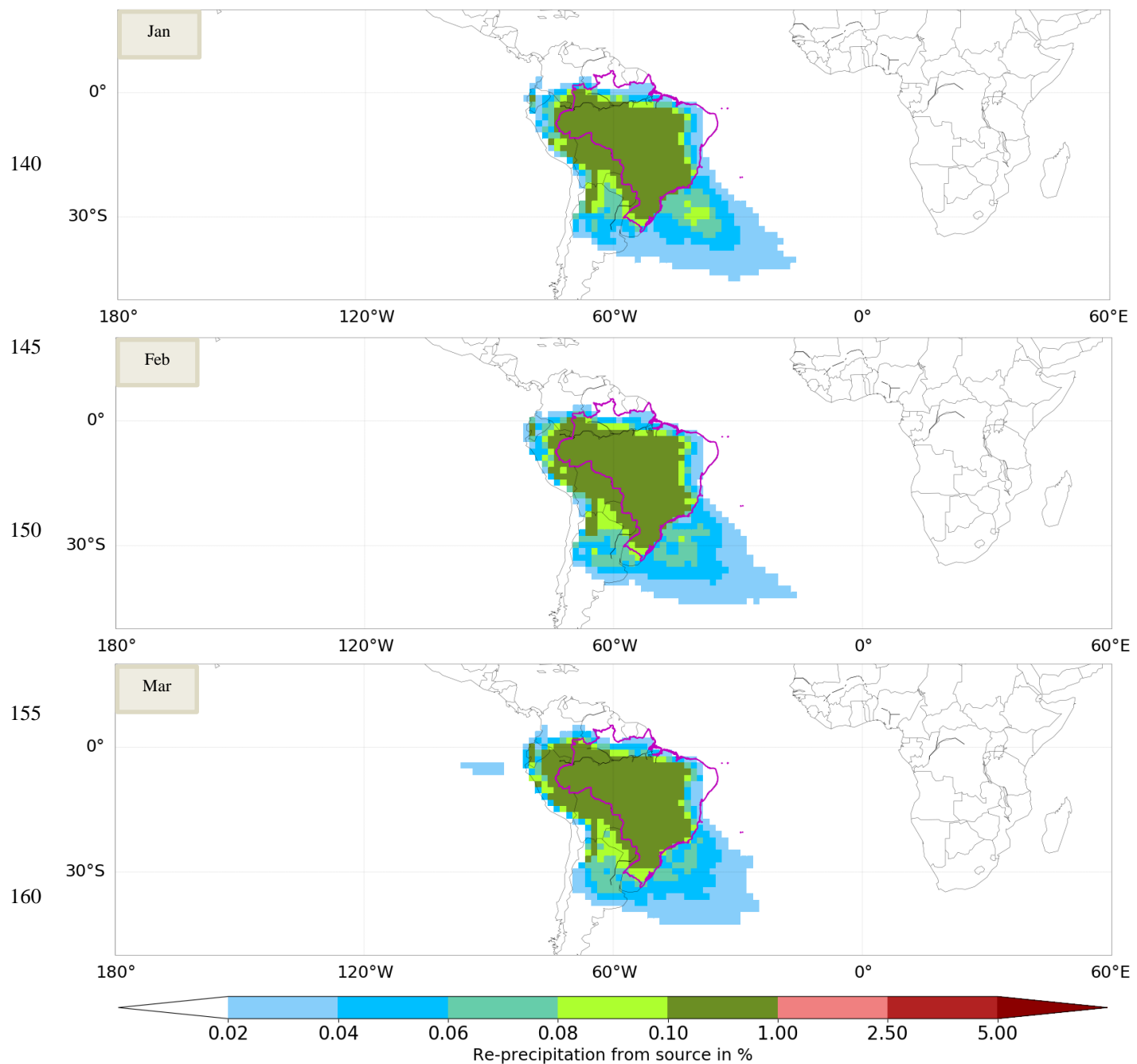


Figure S12 Monthly evaporationsheds (Oct = October, Nov = November, Dec = December) for the grid cell at 0.0° latitude & 33.0° E longitude (Kampala, Uganda), E_{input} : 97.4 mm/month (Oct) / 92.8 mm/month (Nov) / 95.5 mm/month (Dec), Unassigned : 0.0 % (Oct) / 0.0 % (Nov) / 0.0 % (Dec), Colored area covers 94.2 % (Oct) / 94.2 % (Nov) / 93.1 % (Dec) of the assigned water



165 **Figure S13 Monthly evaporation sheds (Jan = January, Feb = February, Mar = March) for Brazil , E_{input} : 118.3 mm/month (Jan) / 107.7 mm/month (Feb) / 115.1 mm/month (Mar), Unassigned : 0.1 % (Jan) / 0.1 % (Feb) / 0.1 % (Mar), Colored area covers 82.9 % (Jan) / 83.4 % (Feb) / 83.9 % (Mar) of the assigned water**

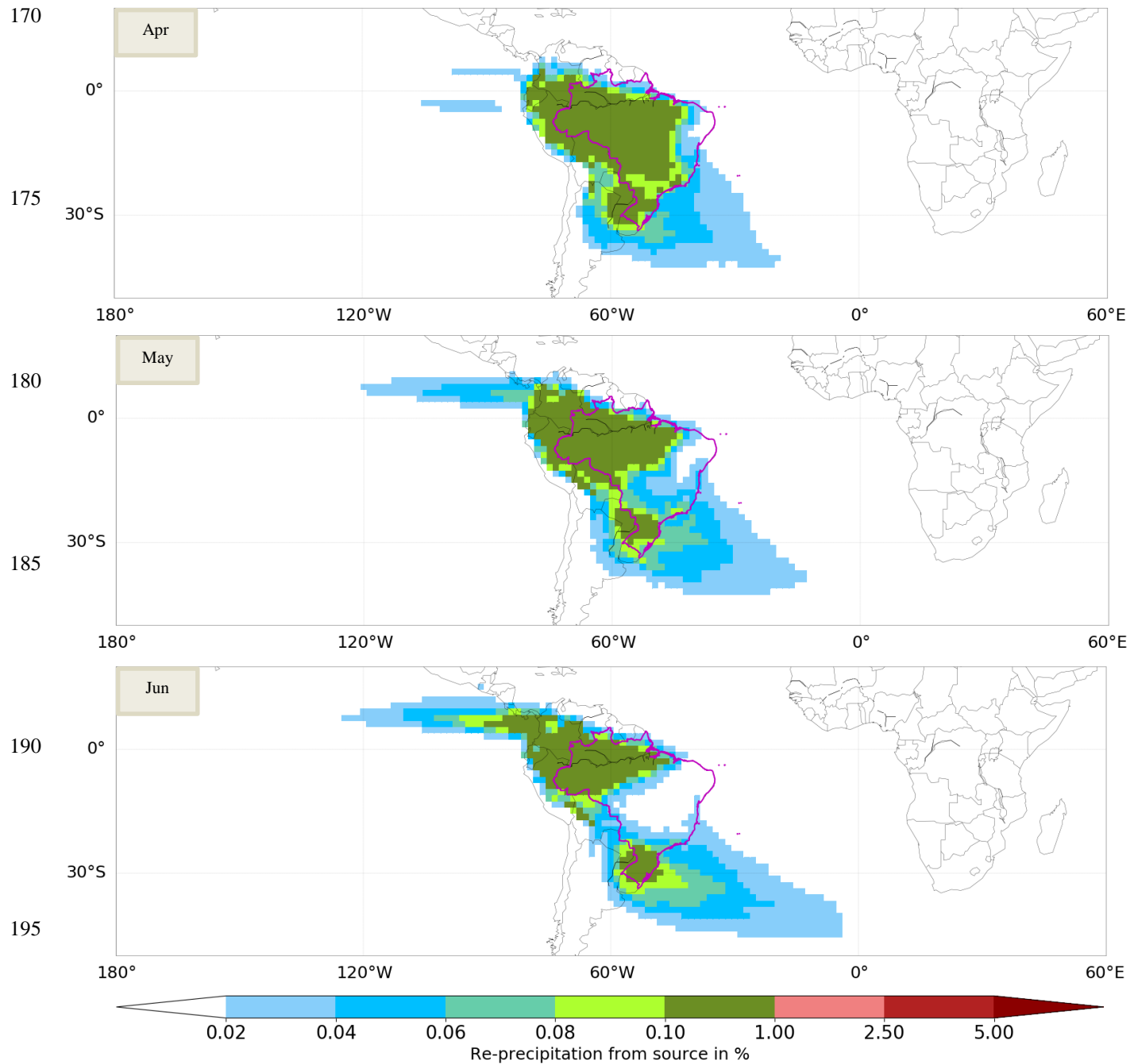


Figure S14 Monthly evaporationsheds (Apr = April, May, Jun = June) for Brazil , E_{input} : 102.5 mm/month (Apr) / 94.2 mm/month (May) / 85.3 mm/month (Jun), Unassigned : 0.1 % (Apr) / 0.0 % (May) / 0.1 % (Jun), Colored area covers 82.9 % (Apr) / 81.9 % (May) / 78.7 % (Jun) of the assigned water

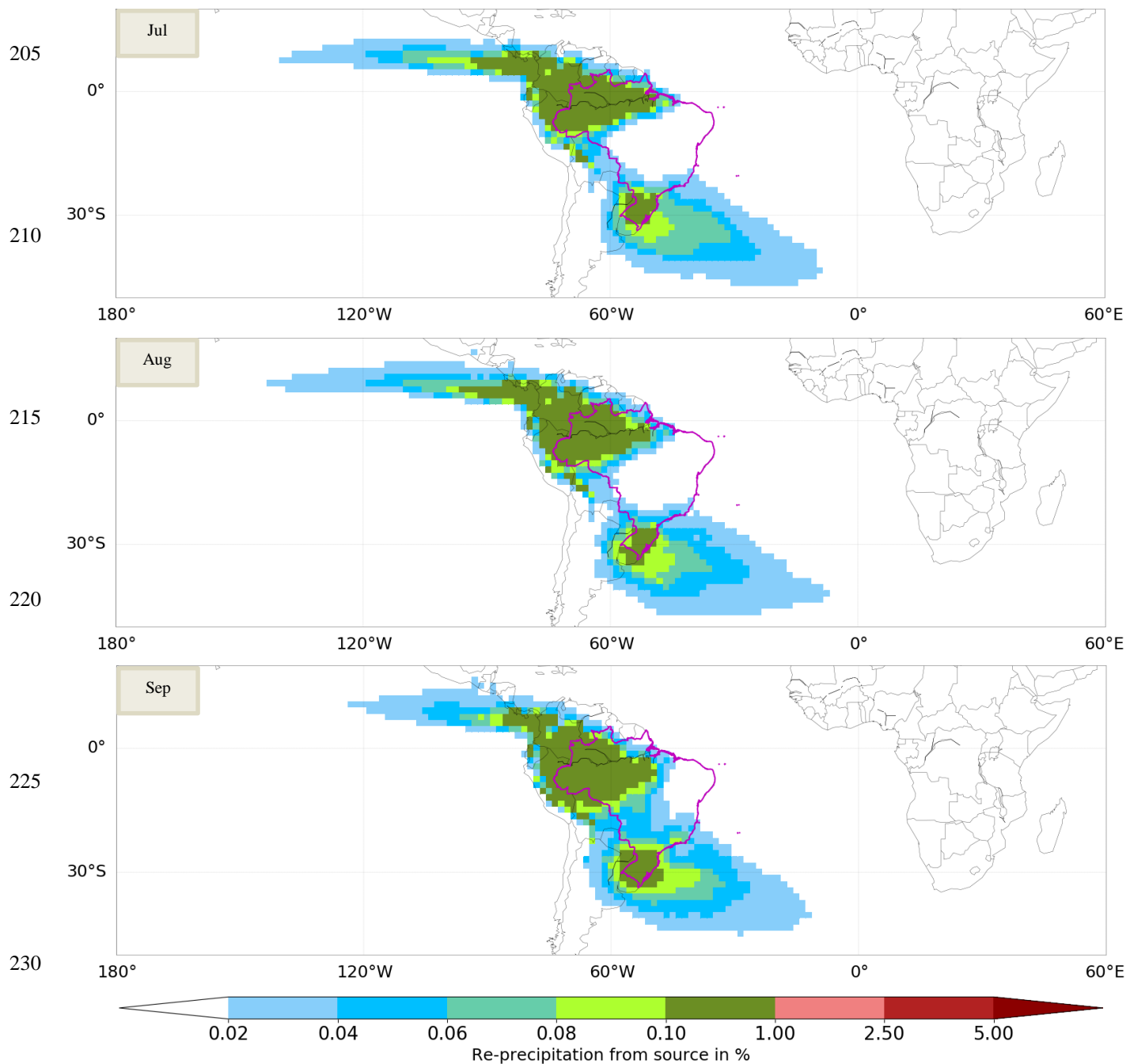


Figure S15 Monthly evaporationsheds (Jul = July, Aug = August, Sep = September) for Brazil , E_{input} : 86.2 mm/month (Jul) / 90.8 mm/month (Aug) / 97.0 mm/month (Sep), Unassigned : 0.1 % (Jul) / 0.1 % (Aug) / 0.1 % (Sep), Colored area covers 76.8 % (Jul) / 77.0 % (Aug) / 78.7 % (Sep) of the assigned water

235

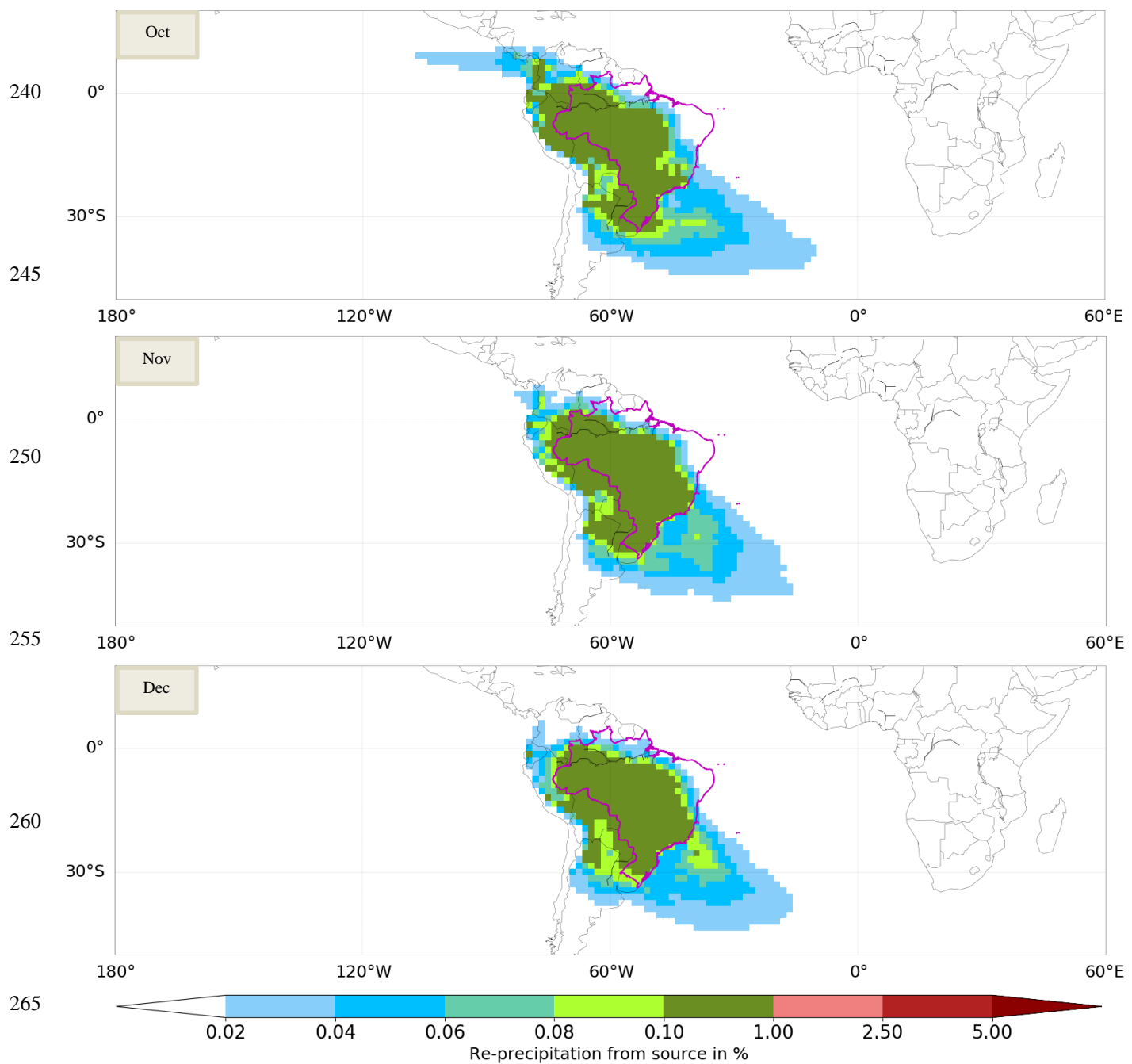


Figure S16 Monthly evaporation sheds (Oct = October, Nov = November, Dec = December) for Brazil , E_{input} : 113.1 mm/month (Oct) / 115.3 mm/month (Nov) / 114.6 mm/month (Dec), Unassigned : 0.1 % (Oct) / 0.1 % (Nov) / 0.1 % (Dec), Colored area covers 81.2 % (Oct) / 83.9 % (Nov) / 84.3 % (Dec) of the assigned water

270

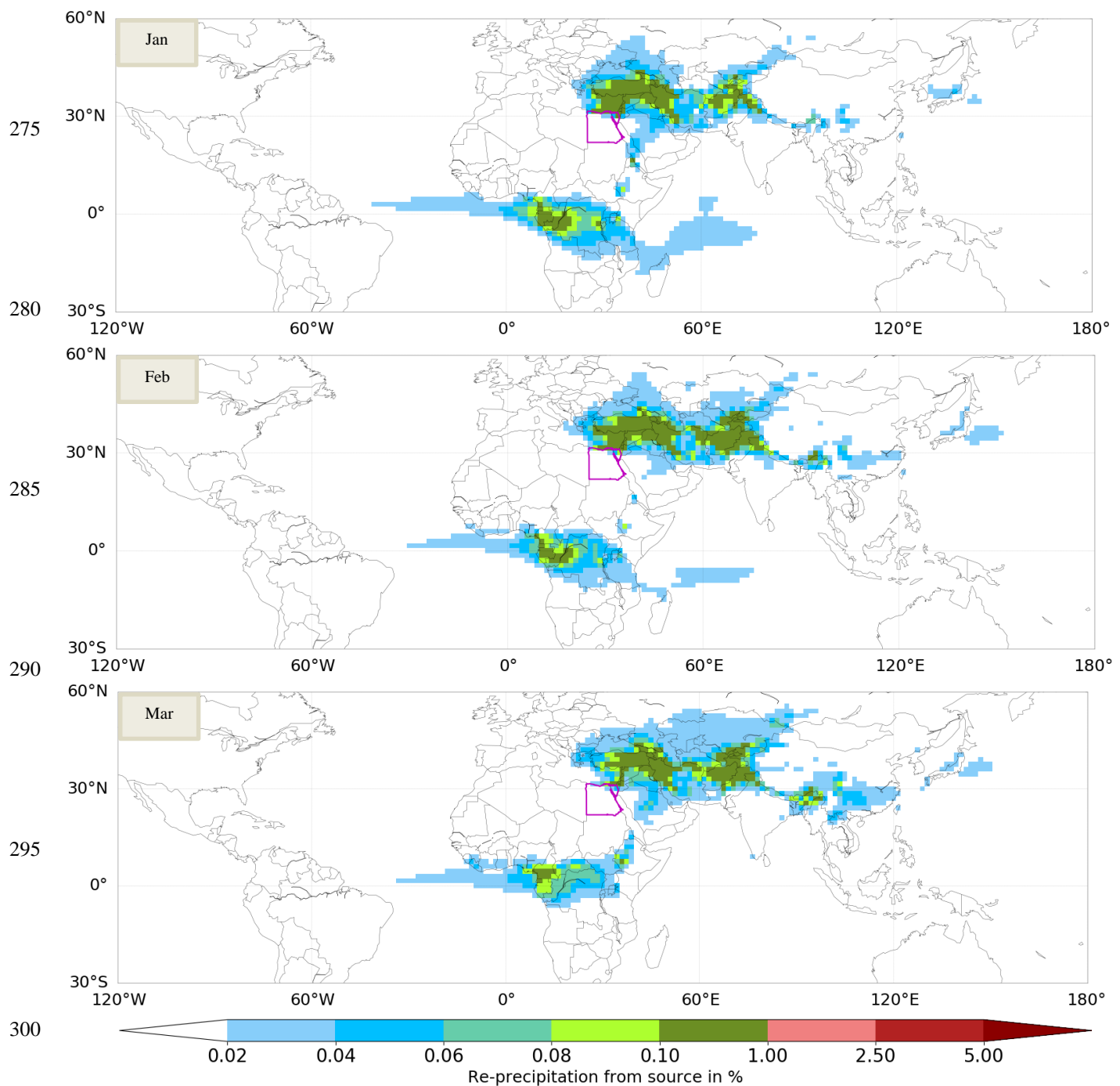


Figure S17 Monthly evaporationsheds (Jan = January, Feb = February, Mar = March) for Egypt , E_{input} : 9.4 mm/month (Jan) / 7.9 mm/month (Feb) / 7.9 mm/month (Mar), Unassigned : 1.1 % (Jan) / 0.8 % (Feb) / 1.2 % (Mar), Colored area covers 61.6 % (Jan) / 61.3 % (Feb) / 62.2 % (Mar) of the assigned water

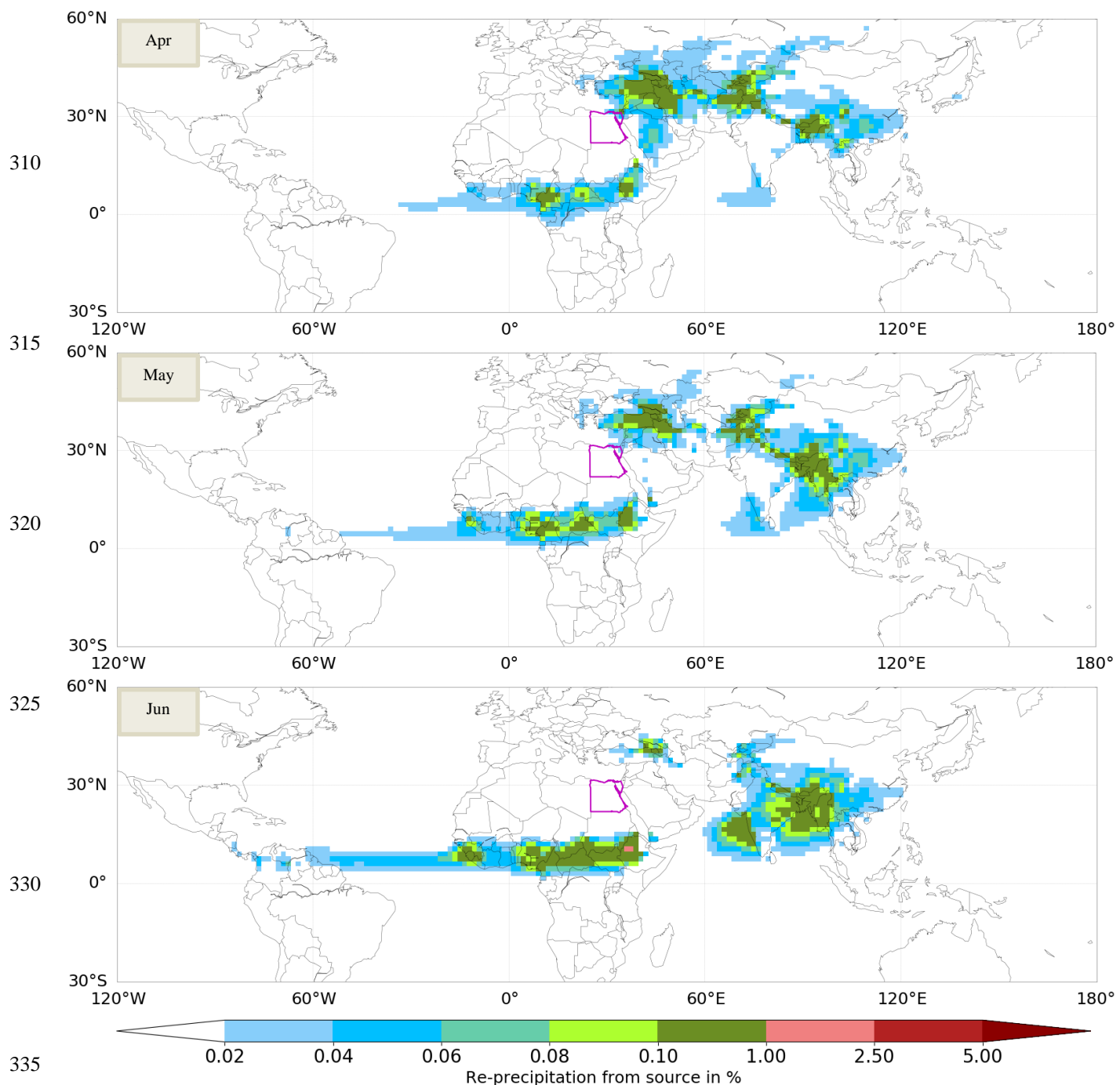


Figure S18 Monthly evaporationsheds (Apr = April, May, Jun = June) for Egypt , E_{input} : 7.3 mm/month (Apr) / 7.6 mm/month (May) / 7.9 mm/month (Jun), Unassigned : 1.1 % (Apr) / 0.9 % (May) / 0.8 % (Jun), Colored area covers 62.6 % (Apr) / 65.0 % (May) / 75.2 % (Jun) of the assigned water

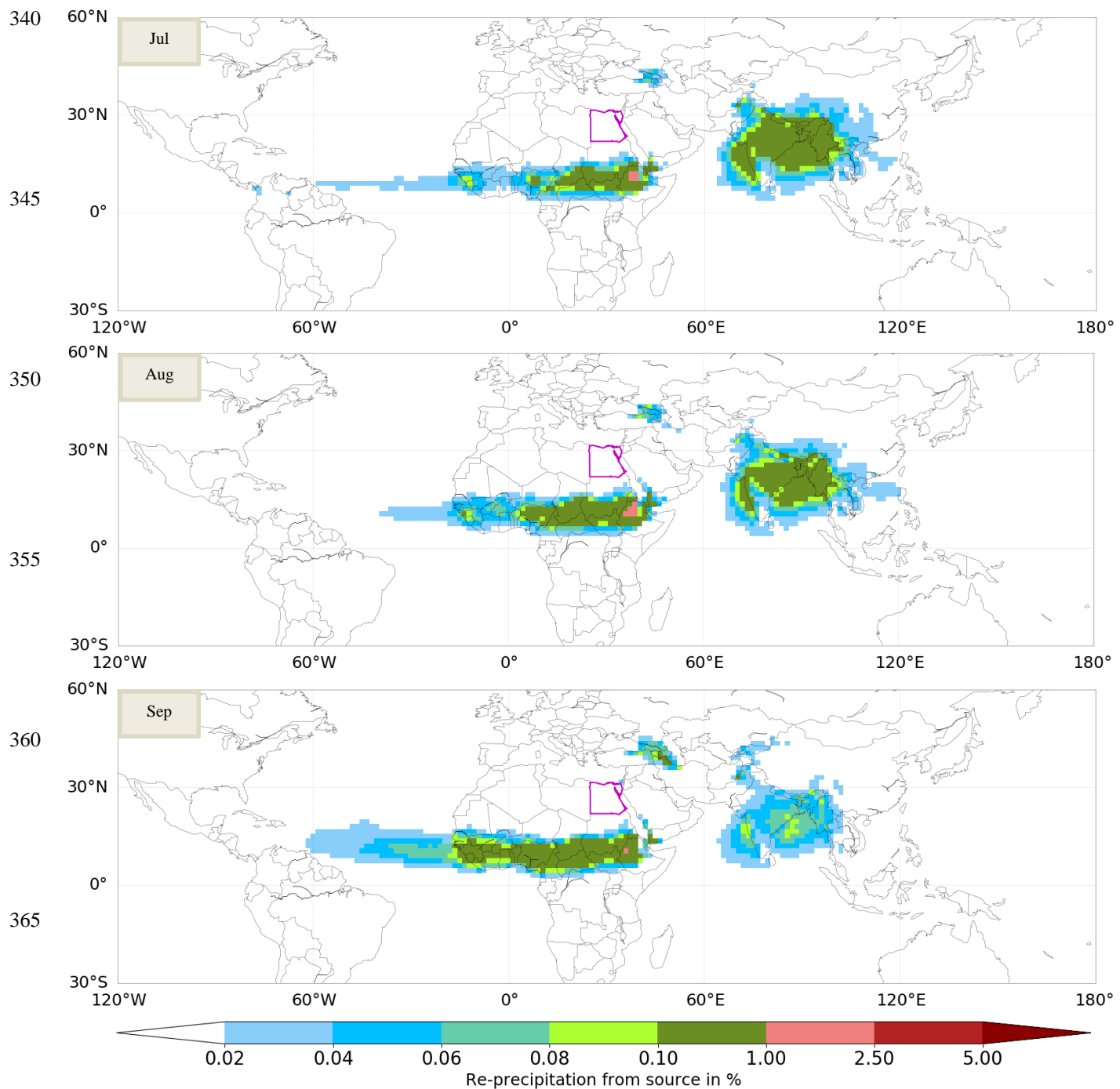


Figure S19 Monthly evaporationsheds (Jul = July, Aug = August, Sep = September) for Egypt , E_{input} : 8.9 mm/month (Jul) / 9.5 mm/month (Aug) / 9.6 mm/month (Sep), Unassigned : 0.3 % (Jul) / 0.3 % (Aug) / 0.5 % (Sep), Colored area covers 80.2 % (Jul) / 80.3 % (Aug) / 74.1 % (Sep) of the assigned water

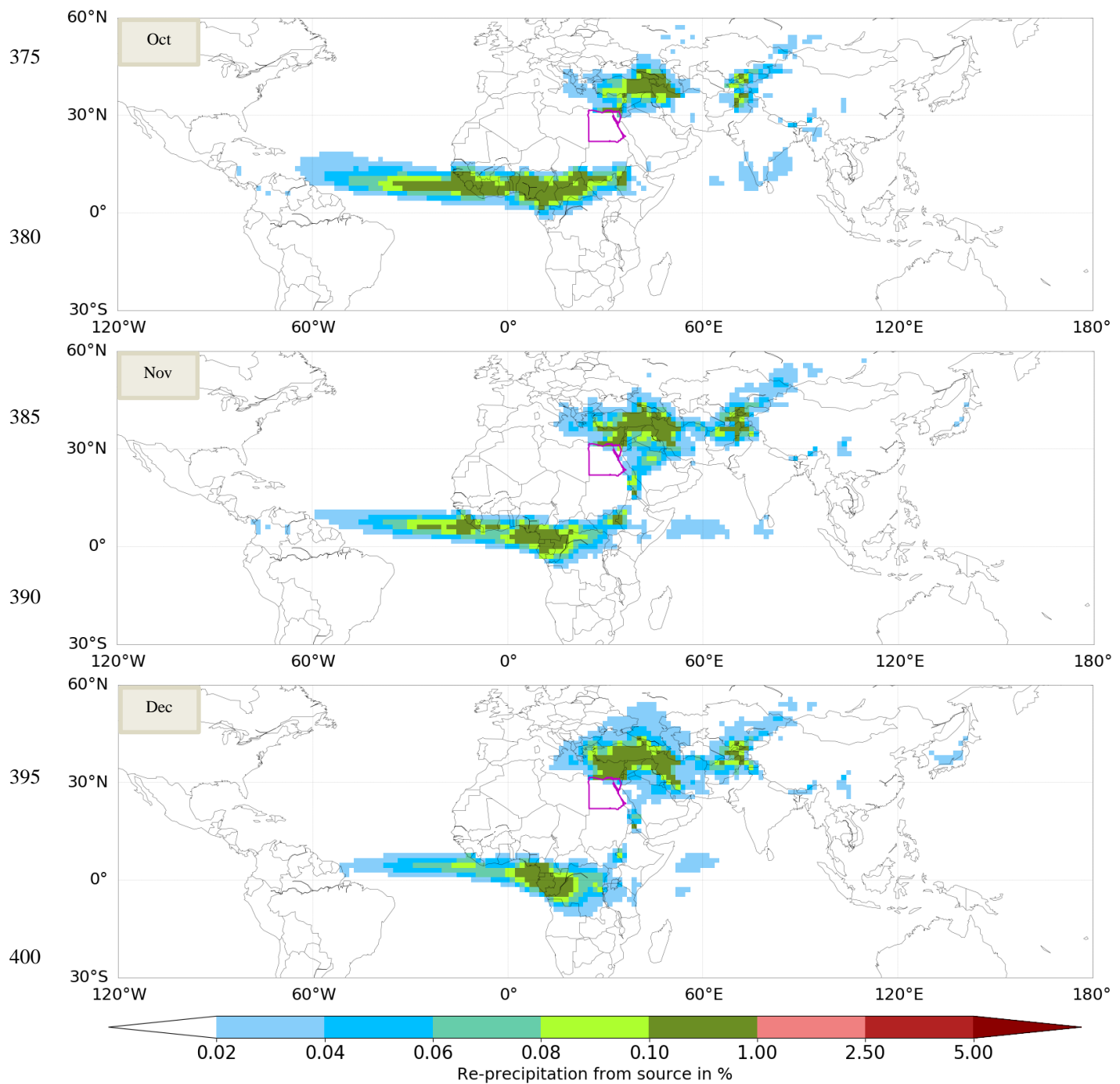


Figure S20 Monthly evaporationsheds (Oct = October, Nov = November, Dec = December) for Egypt , E_{input} : 9.5 mm/month (Oct) / 9.2 mm/month (Nov) / 9.5 mm/month (Dec), Unassigned : 0.9 % (Oct) / 1.0 % (Nov) / 1.0 % (Dec), Colored area covers 58.5 % (Oct) / 59.1 % (Nov) / 62.1 % (Dec) of the assigned water

405

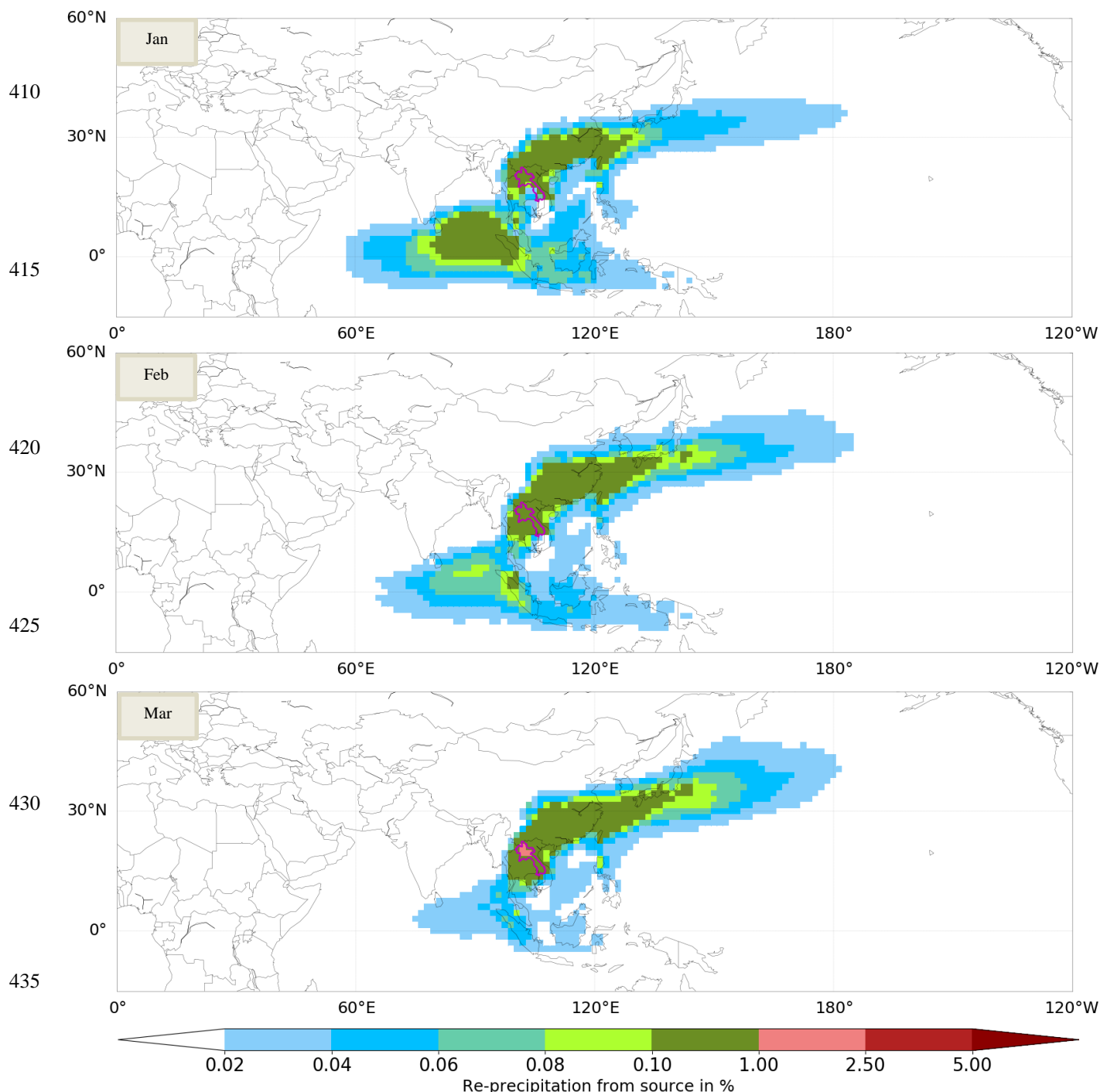


Figure S21 Monthly evaporationsheds (Jan = January, Feb = February, Mar = March) for Laos , E_{input} : 67.0 mm/month (Jan) / 75.1 mm/month (Feb) / 105.3 mm/month (Mar), Unassigned : 0.1 % (Jan) / 0.1 % (Feb) / 0.2 % (Mar), Colored area covers 77.2 % (Jan) / 76.3 % (Feb) / 77.5 % (Mar) of the assigned water

440

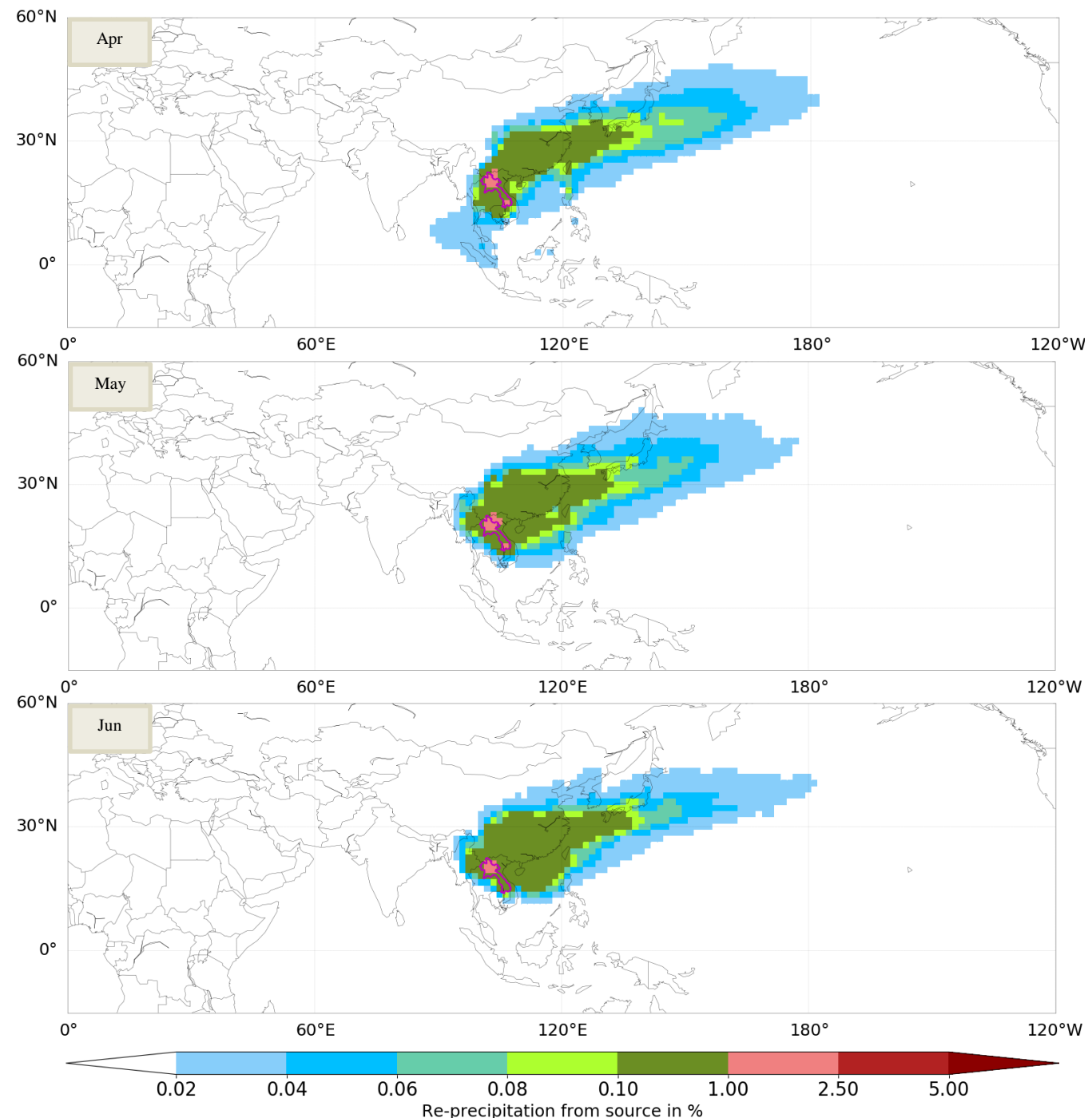


Figure S22 Monthly evaporationsheds (Apr = April, May, Jun = June) for Laos , E_{input} : 123.3 mm/month (Apr) / 123.1 mm/month (May) / 112.7 mm/month (Jun), Unassigned : 0.3 % (Apr) / 0.7 % (May) / 0.6 % (Jun), Colored area covers 80.3 % (Apr) / 82.2 % (May) / 82.1 % (Jun) of the assigned water

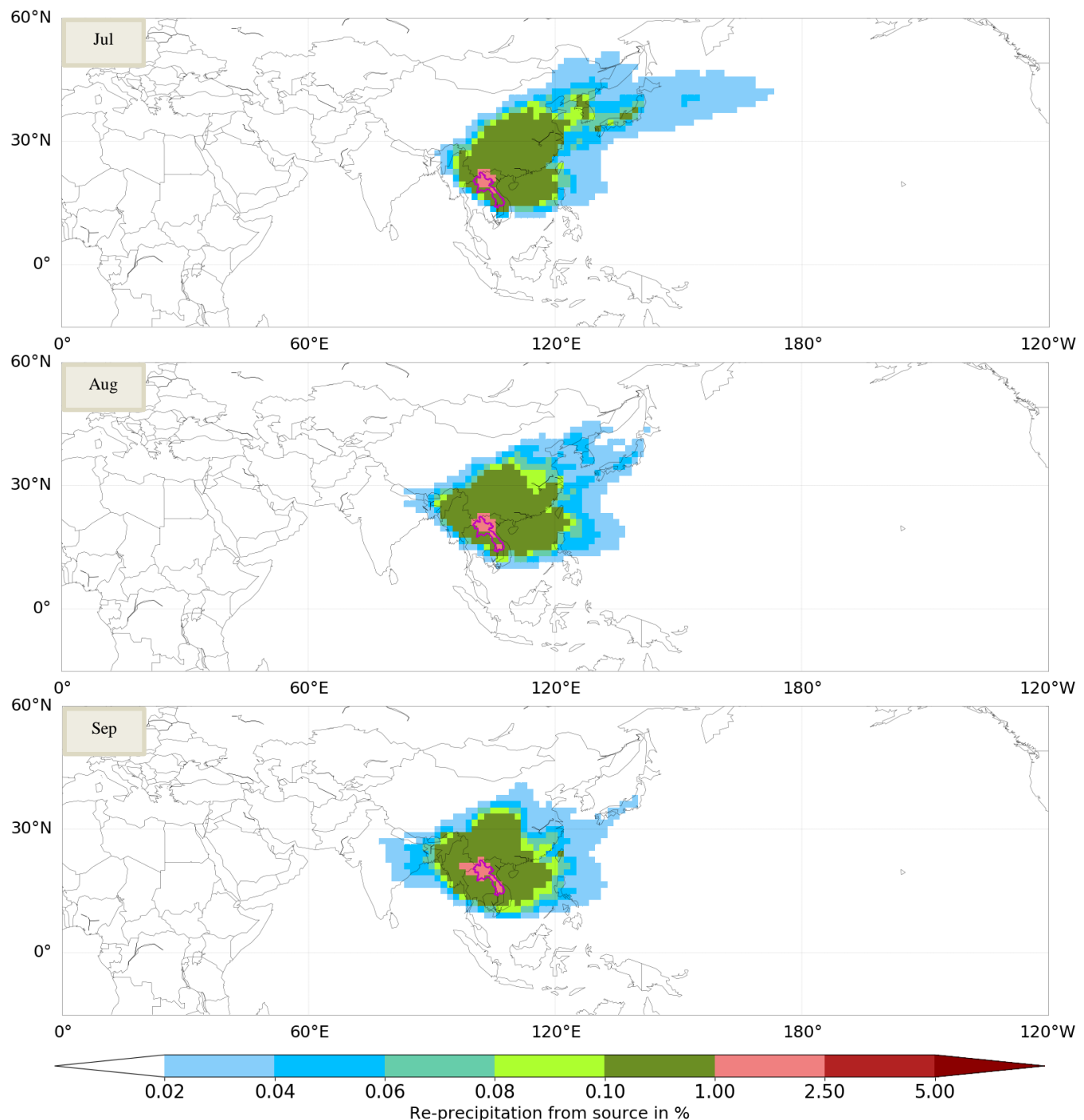


Figure S23 Monthly evaporationsheds (Jul = July, Aug = August, Sep = September) for Laos , E_{input} : 106.0 mm/month (Jul) / 107.0 mm/month (Aug) / 104.1 mm/month (Sep), Unassigned : 1.1 % (Jul) / 0.6 % (Aug) / 0.2 % (Sep), Colored area covers 79.7 % (Jul) / 82.8 % (Aug) / 87.9 % (Sep) of the assigned water

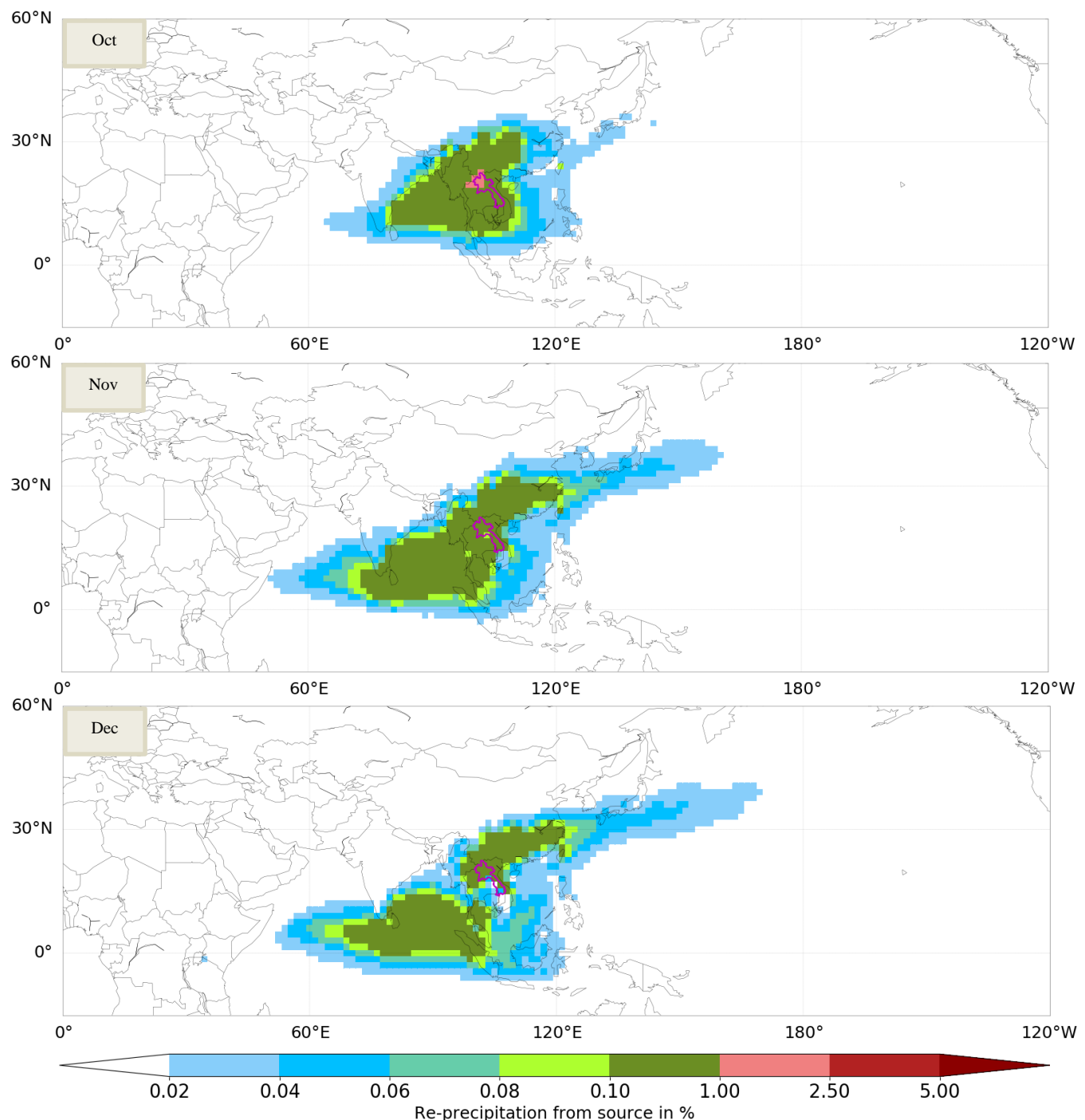


Figure S24 Monthly evaporationsheds (Oct = October, Nov = November, Dec = December) for Laos , E_{input} : 105.0 mm/month (Oct) / 84.6 mm/month (Nov) / 65.8 mm/month (Dec), Unassigned : 0.1 % (Oct) / 0.1 % (Nov) / 0.1 % (Dec), Colored area covers 87.7 % (Oct) / 84.6 % (Nov) / 79.8 % (Dec) of the assigned water

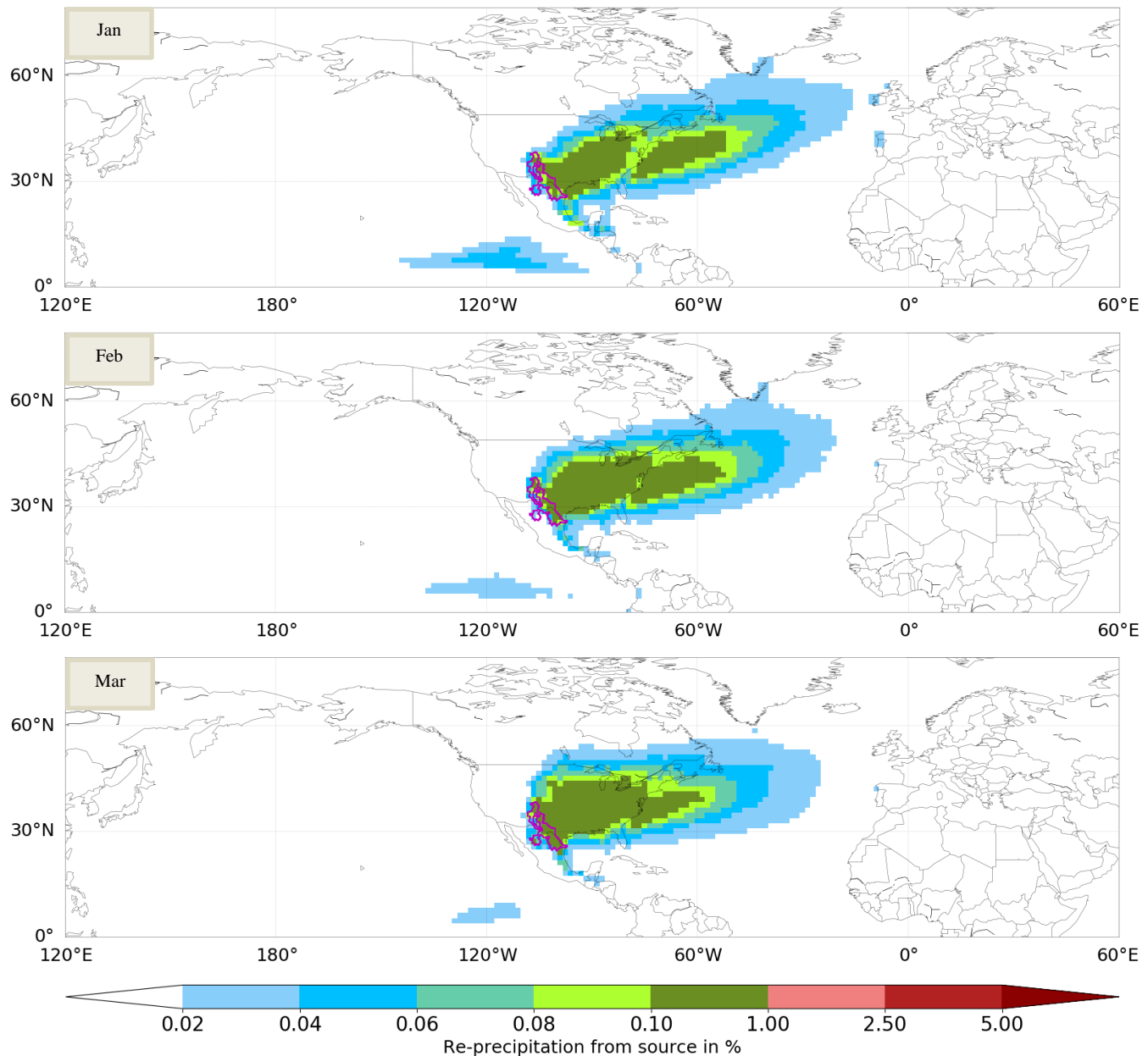


Figure S25 Monthly evaporationsheds (Jan = January, Feb = February, Mar = March) for the basin with the ID 1463188 (part of the Rio Grande basin), E_{input} : 19.5 mm/month (Jan) / 21.9 mm/month (Feb) / 32.9 mm/month (Mar), Unassigned : 0.8 % (Jan) / 0.7 % (Feb) / 0.6 % (Mar), Colored area covers 73.6 % (Jan) / 74.4 % (Feb) / 74.0 % (Mar) of the assigned water

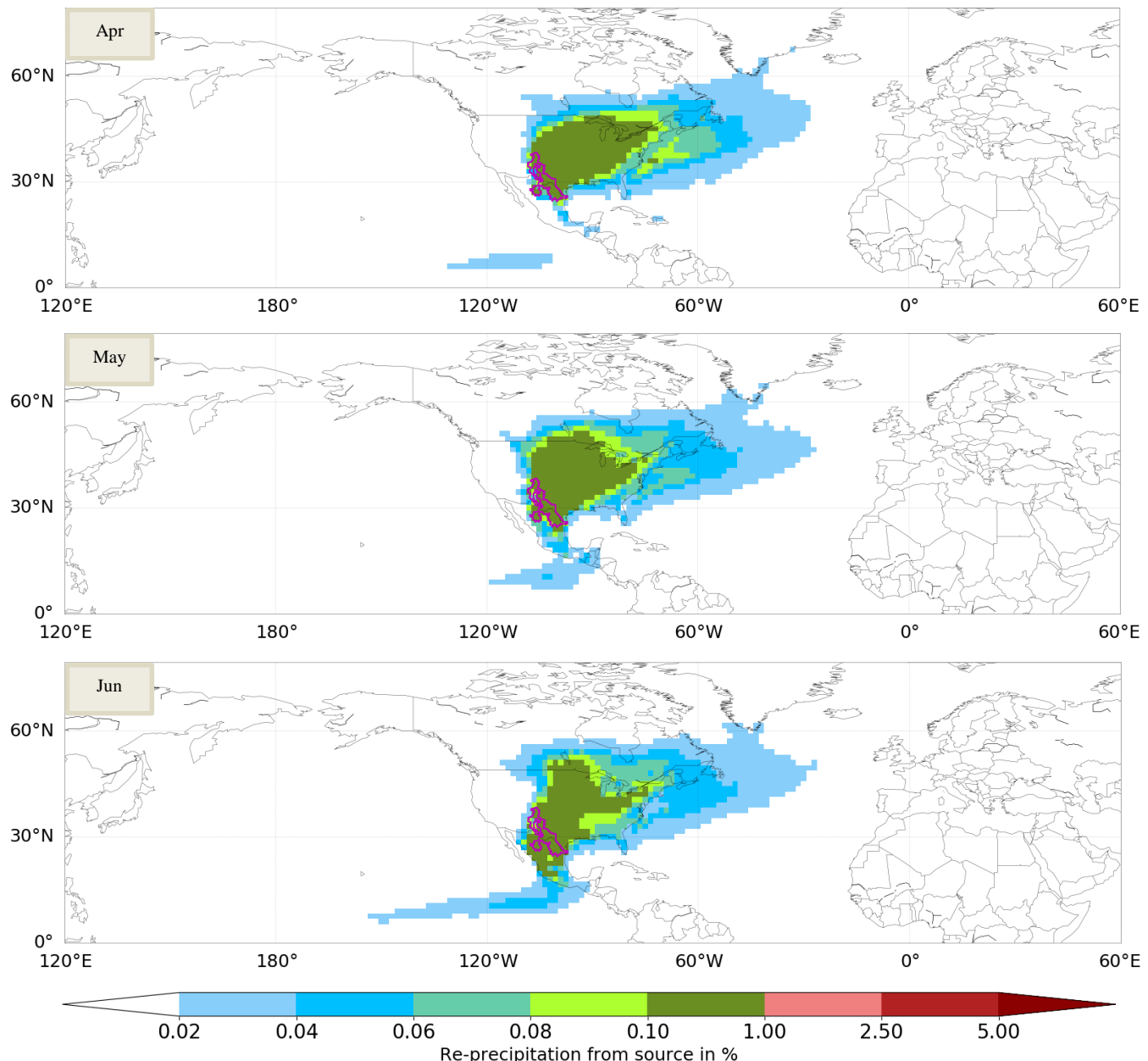


Figure S26 Monthly evaporationsheds (Apr = April, May, Jun = June) for the basin with the ID 1463188 (part of the Rio Grande basin), E_{input} : 40.7 mm/month (Apr) / 52.3 mm/month (May) / 50.1 mm/month (Jun), Unassigned : 0.9 % (Apr) / 1.1 % (May) / 1.7 % (Jun), Colored area covers 74.6 % (Apr) / 76.4 % (May) / 73.1 % (Jun) of the assigned water

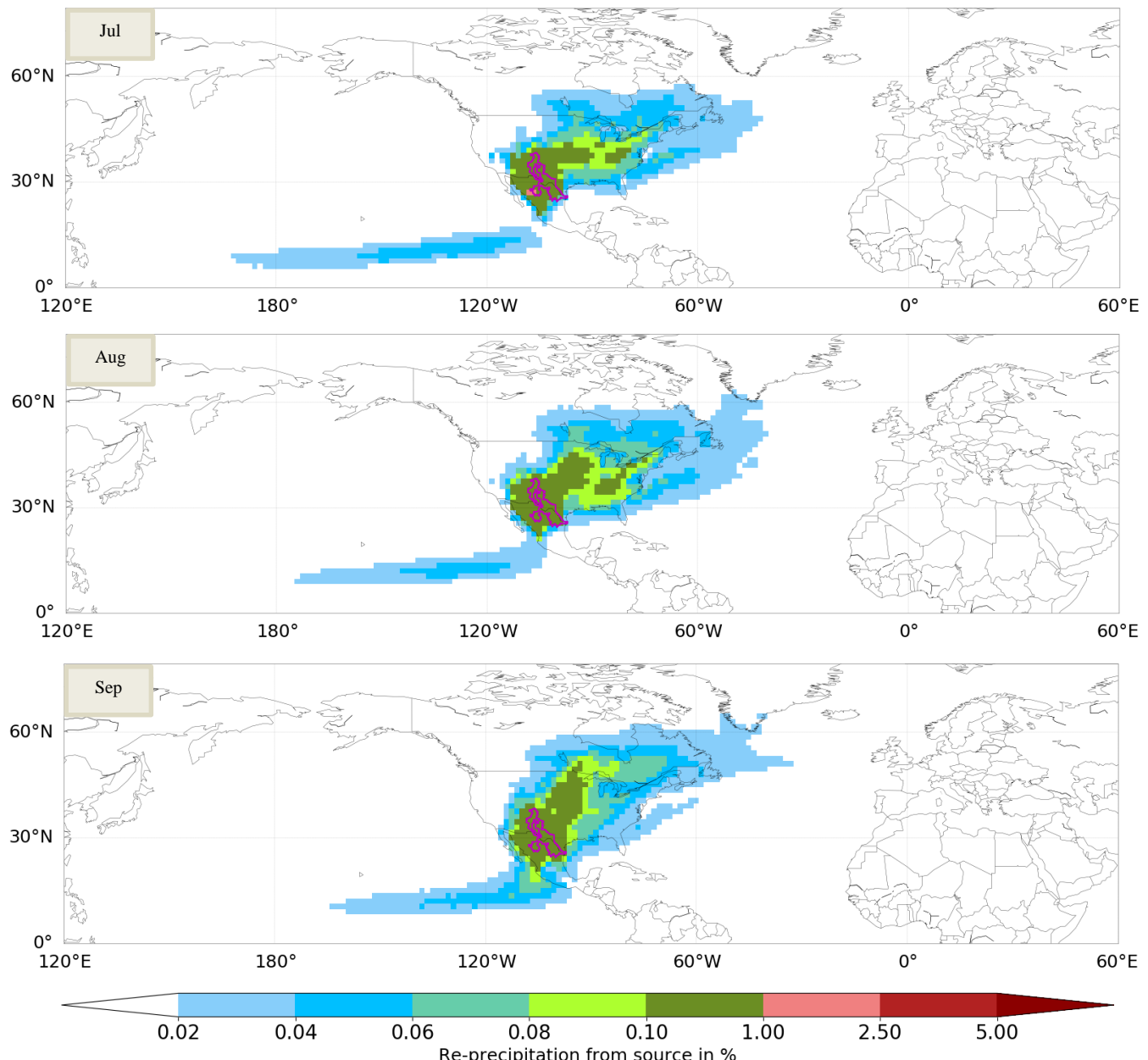


Figure S27 Monthly evaporationsheds (Jul = July, Aug = August, Sep = September) for the basin with the ID 1463188 (part of the Rio Grande basin), E_{input} : 67.1 mm/month (Jul) / 64.7 mm/month (Aug) / 60.5 mm/month (Sep), Unassigned : 1.5 % (Jul) / 1.5 % (Aug) / 1.6 % (Sep), Colored area covers 69.1 % (Jul) / 69.7 % (Aug) / 69.9 % (Sep) of the assigned water

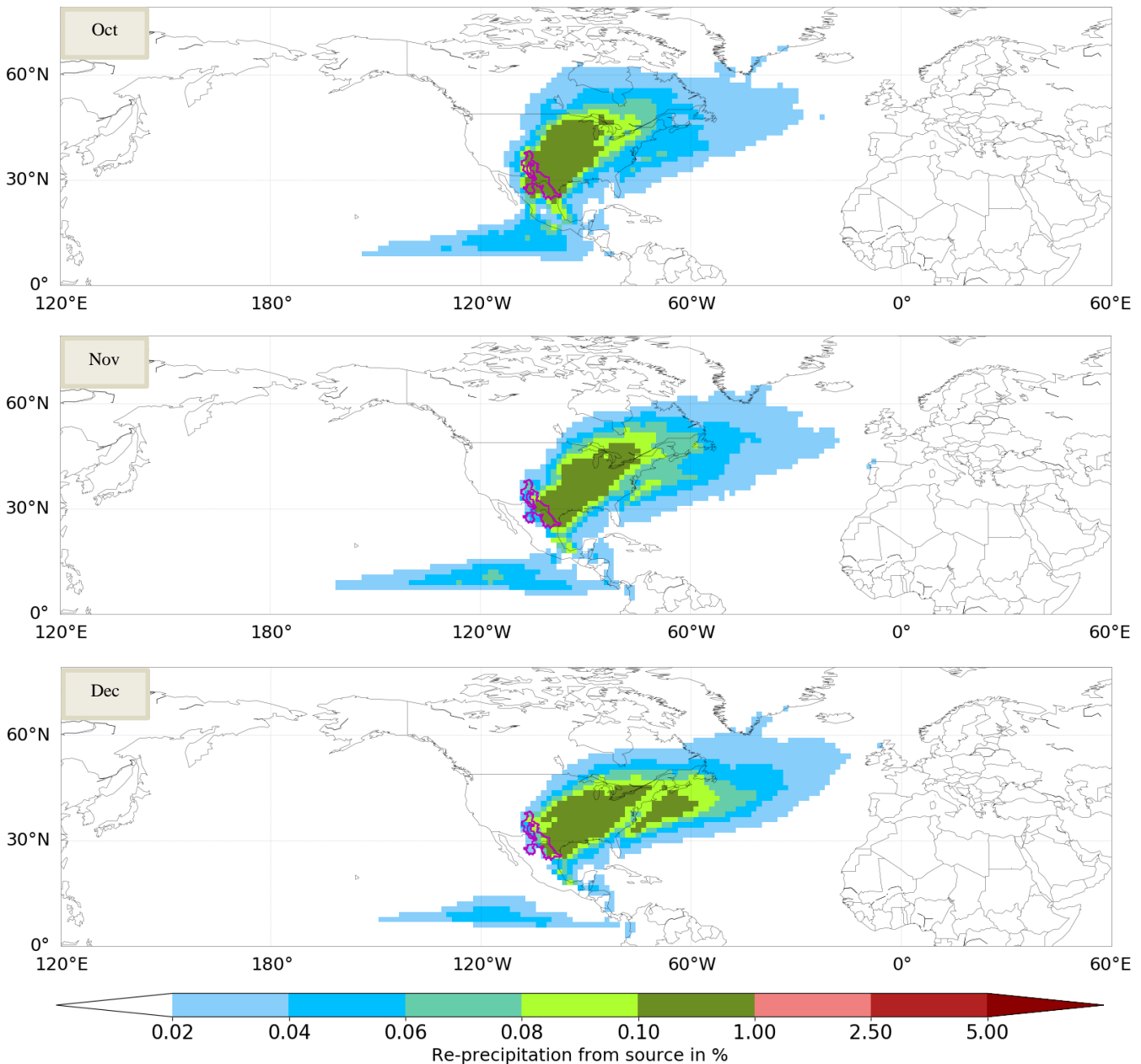


Figure S28 Monthly evaporationsheds (Oct = October, Nov = November, Dec = December) for the basin with the ID 1463188 (part of the Rio Grande basin), E_{input} : 47.1 mm/month (Oct) / 26.1 mm/month (Nov) / 19.6 mm/month (Dec), Unassigned : 1.6 % (Oct) / 1.0 % (Nov) / 0.8 % (Dec), Colored area covers 71.3 % (Oct) / 71.2 % (Nov) / 73.1 % (Dec) of the assigned water

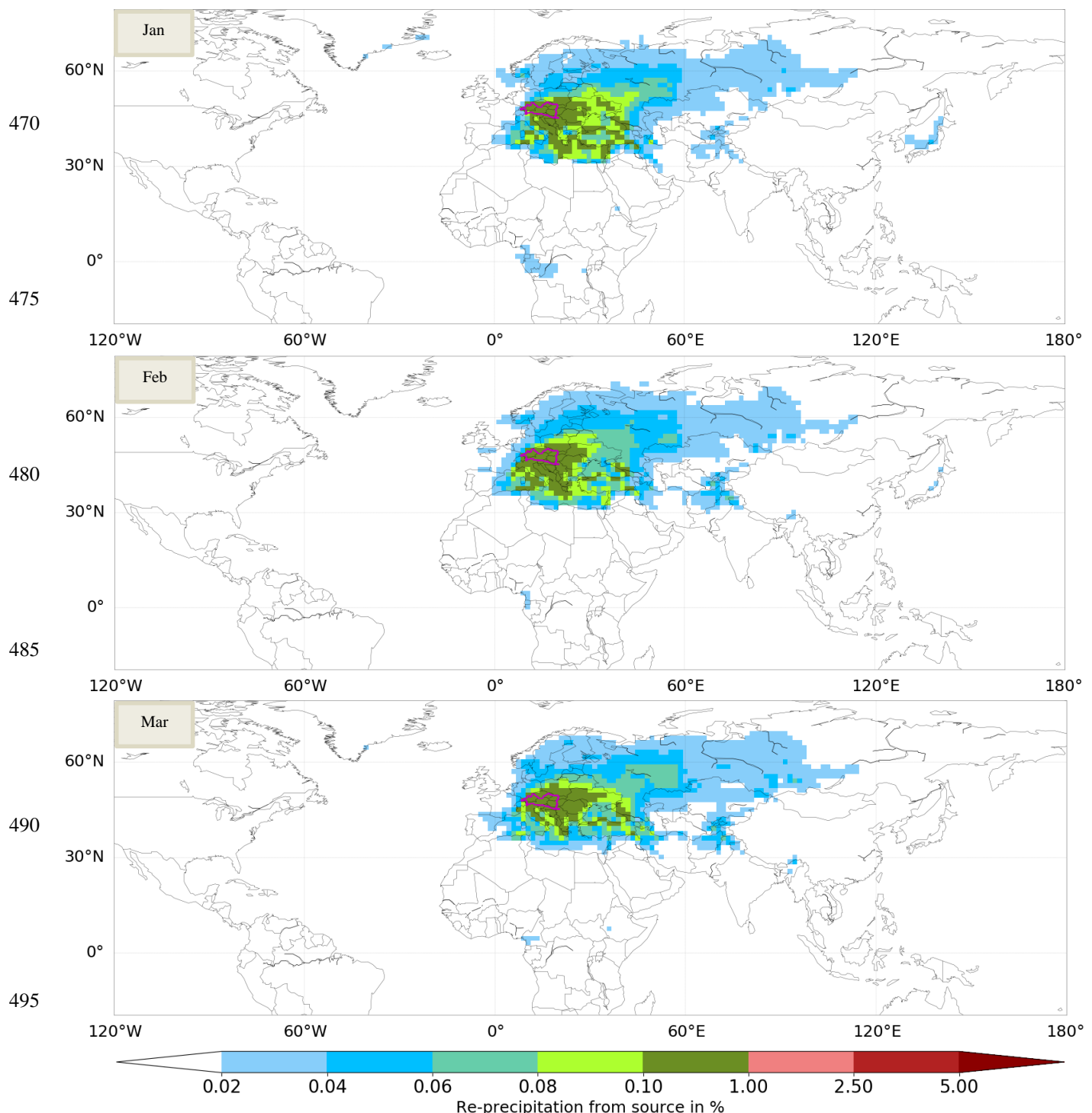
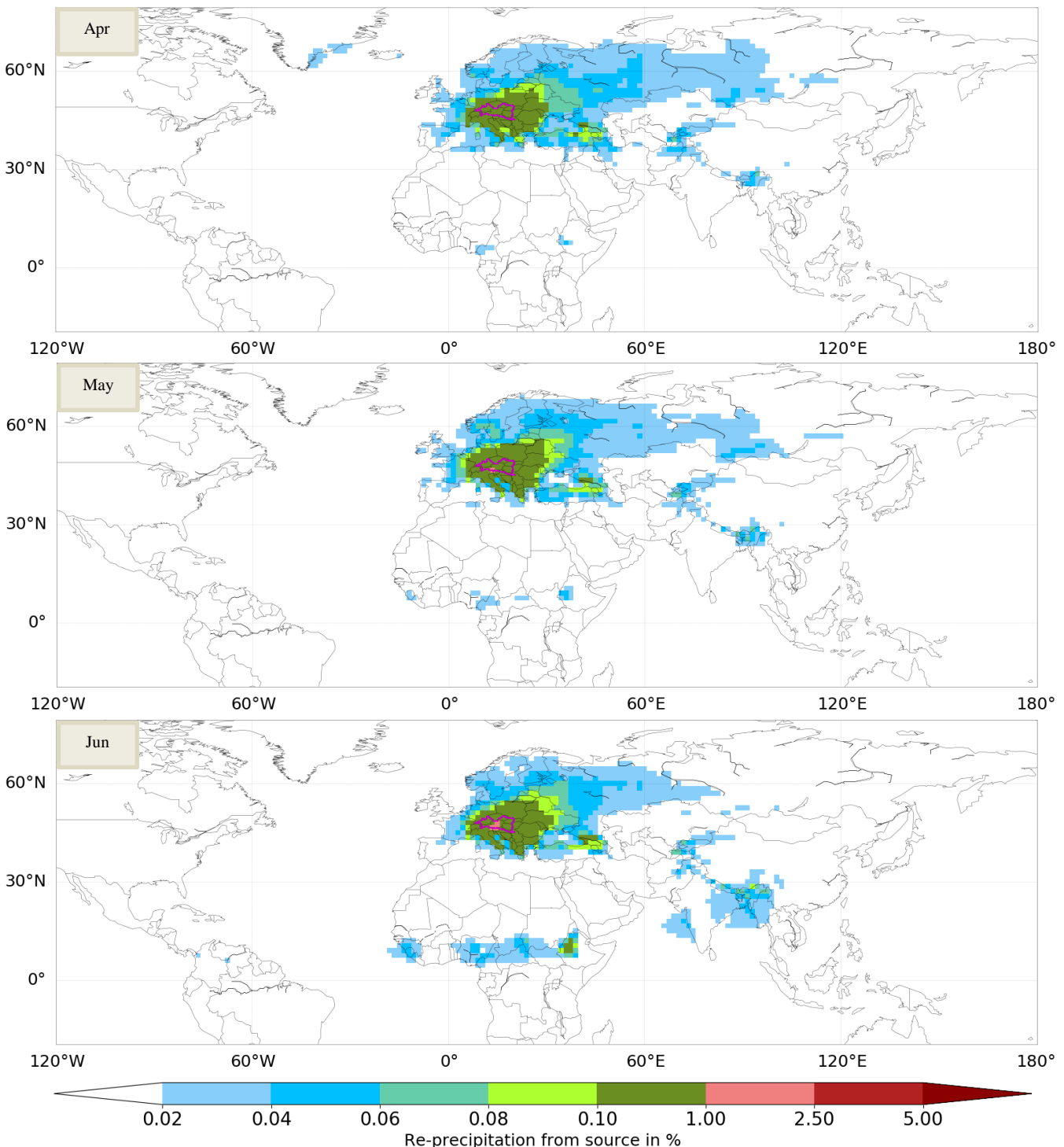


Figure S29 Monthly evaporationsheds (Jan = January, Feb = February, Mar = March) for the basin with the ID 1019324 (part of the Danube basin), E_{input} : 10.4 mm/month (Jan) / 15.9 mm/month (Feb) / 36.2 mm/month (Mar), Unassigned : 3.7 % (Jan) / 3.8 % (Feb) / 3.4 % (Mar), Colored area covers 65.4 % (Jan) / 68.0 % (Feb) / 68.8 % (Mar) of the assigned water



500 **Figure S30 Monthly evaporation sheds (Apr = April, May, Jun = June) for the basin with the ID 1019324 (part of the Danube basin),**
 $E_{\text{input}} : 61.6 \text{ mm/month (Apr)} / 87.7 \text{ mm/month (May)} / 99.3 \text{ mm/month (Jun)}$, Unassigned : 4.6 % (Apr) / 3.6 % (May) / 3.6 % (Jun),
Colored area covers 66.4 % (Apr) / 65.8 % (May) / 69.3 % (Jun) of the assigned water

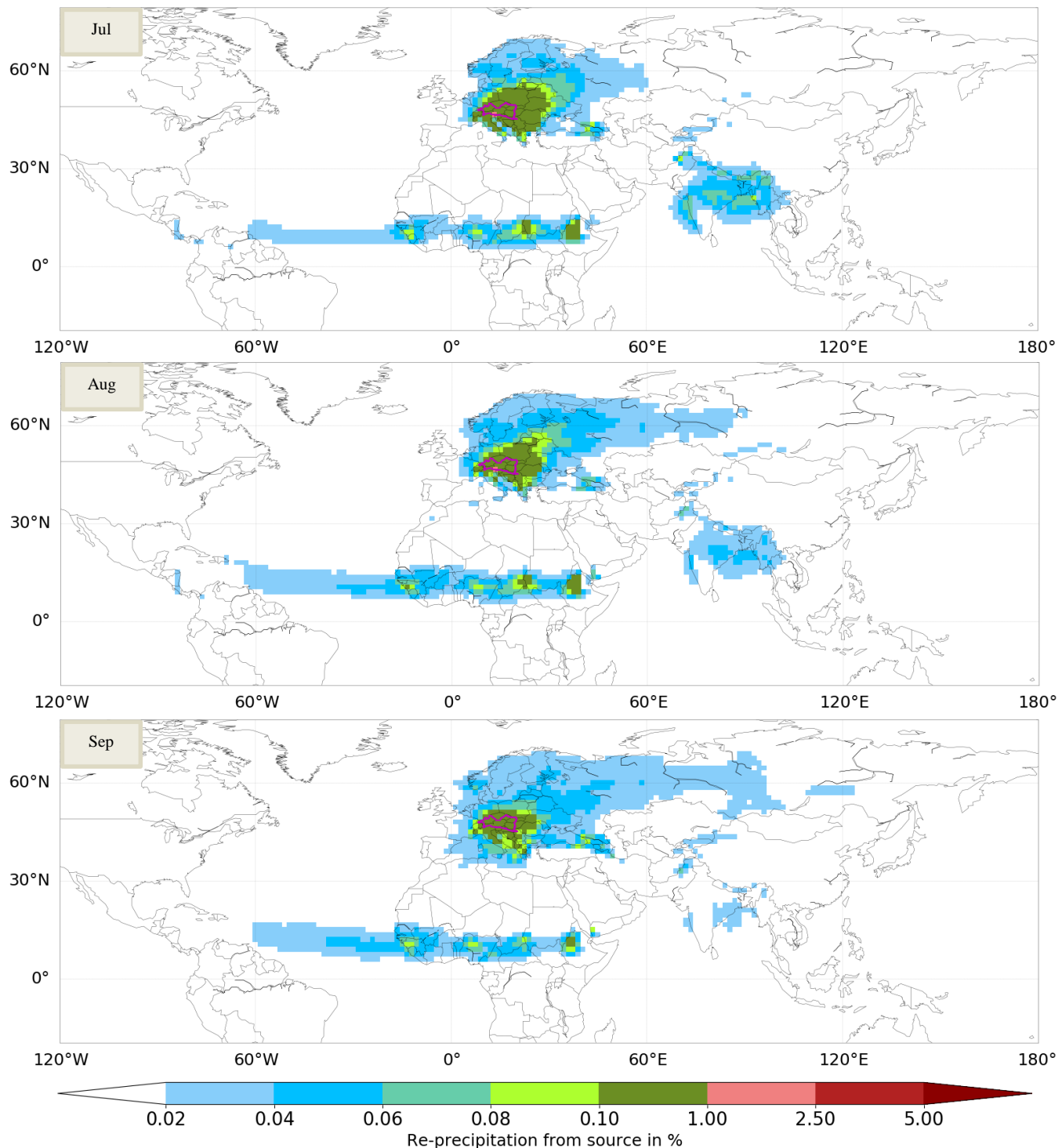


Figure S31 Monthly evaporationsheds (Jul = July, Aug = August, Sep = September) for the basin with the ID 1019324 (part of the Danube basin), E_{input} : 103.0 mm/month (Jul) / 85.7 mm/month (Aug) / 53.2 mm/month (Sep), Unassigned : 3.5 % (Jul) / 3.8 % (Aug) / 6.0 % (Sep), Colored area covers 69.5 % (Jul) / 66.5 % (Aug) / 59.6 % (Sep) of the assigned water

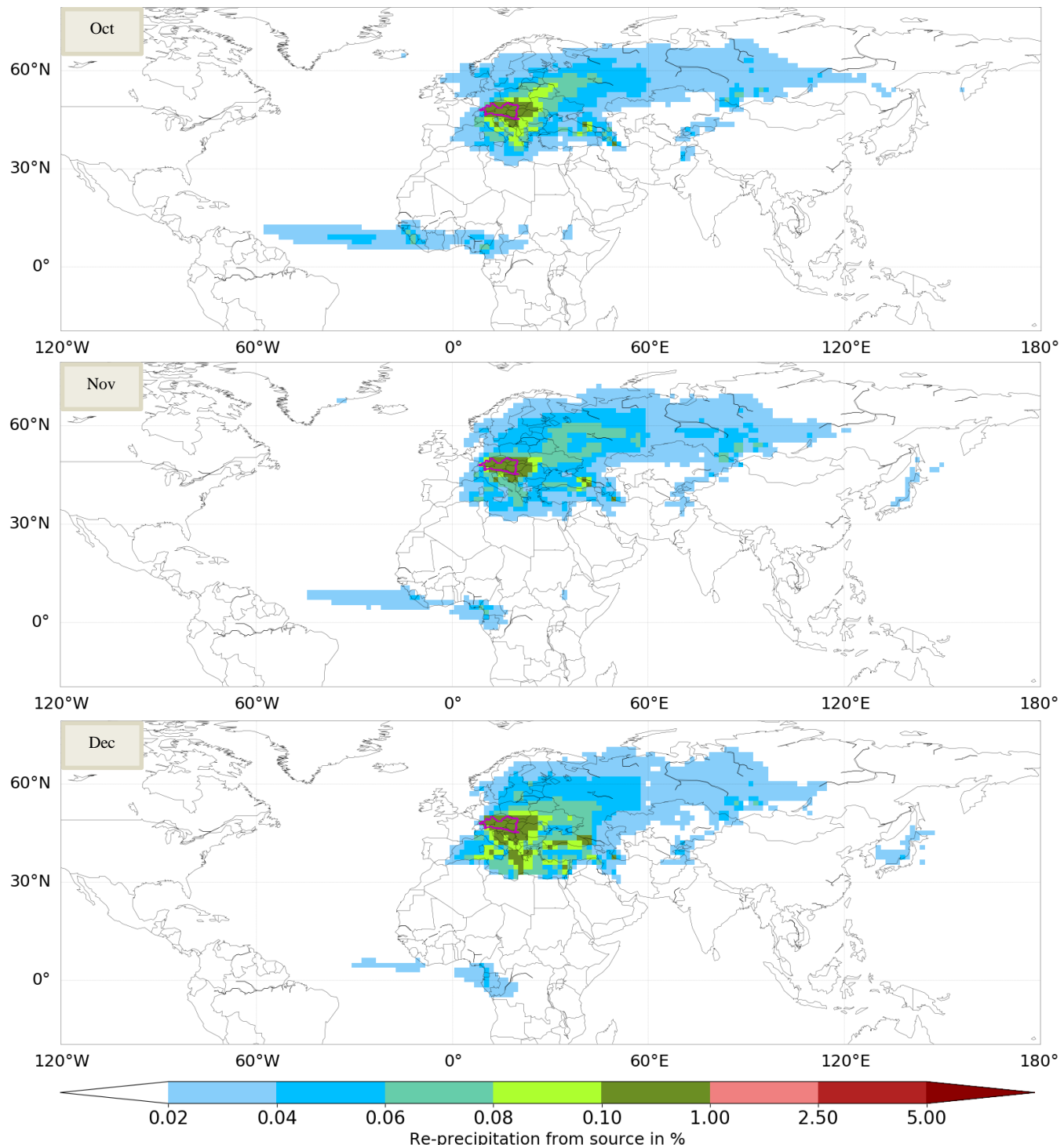


Figure S32 Monthly evaporationsheds (Oct = October, Nov = November, Dec = December) for the basin with the ID 1019324 (part of the Danube basin), E_{input} : 31.5 mm/month (Oct) / 15.5 mm/month (Nov) / 9.5 mm/month (Dec), Unassigned : 4.2 % (Oct) / 4.3 % (Nov) / 4.0 % (Dec), Colored area covers 55.6 % (Oct) / 57.8 % (Nov) / 62.2 % (Dec) of the assigned water

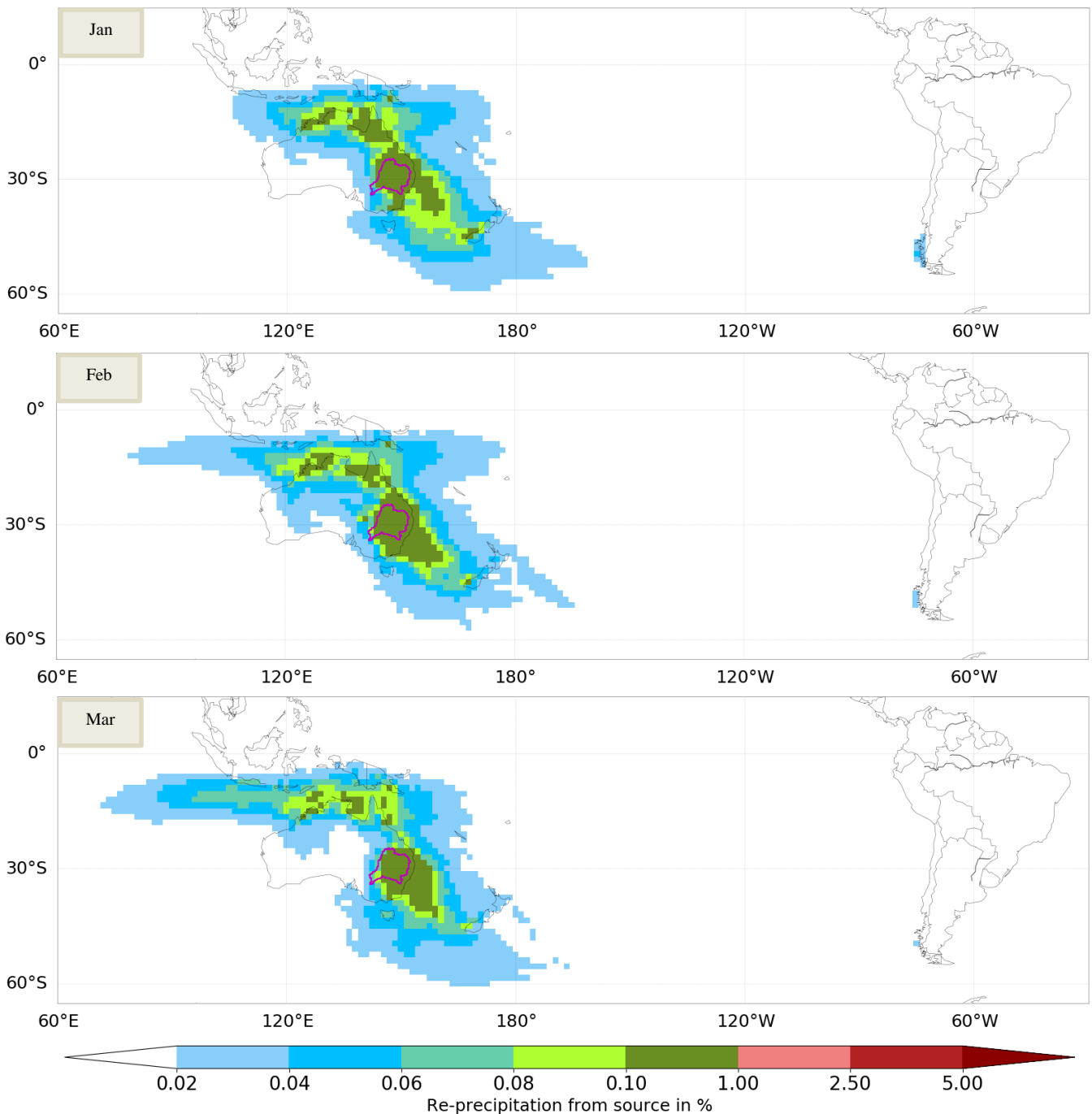


Figure S33 Monthly evaporationsheds (Jan = January, Feb = February, Mar = March) for the basin with the ID 2245569 (part of the Murray-Darling basin), E_{input} : 67.3 mm/month (Jan) / 58.0 mm/month (Feb) / 50.2 mm/month (Mar), Unassigned : 0.6 % (Jan) / 0.4 % (Feb) / 0.5 % (Mar), Colored area covers 62.8 % (Jan) / 63.5 % (Feb) / 62.7 % (Mar) of the assigned water

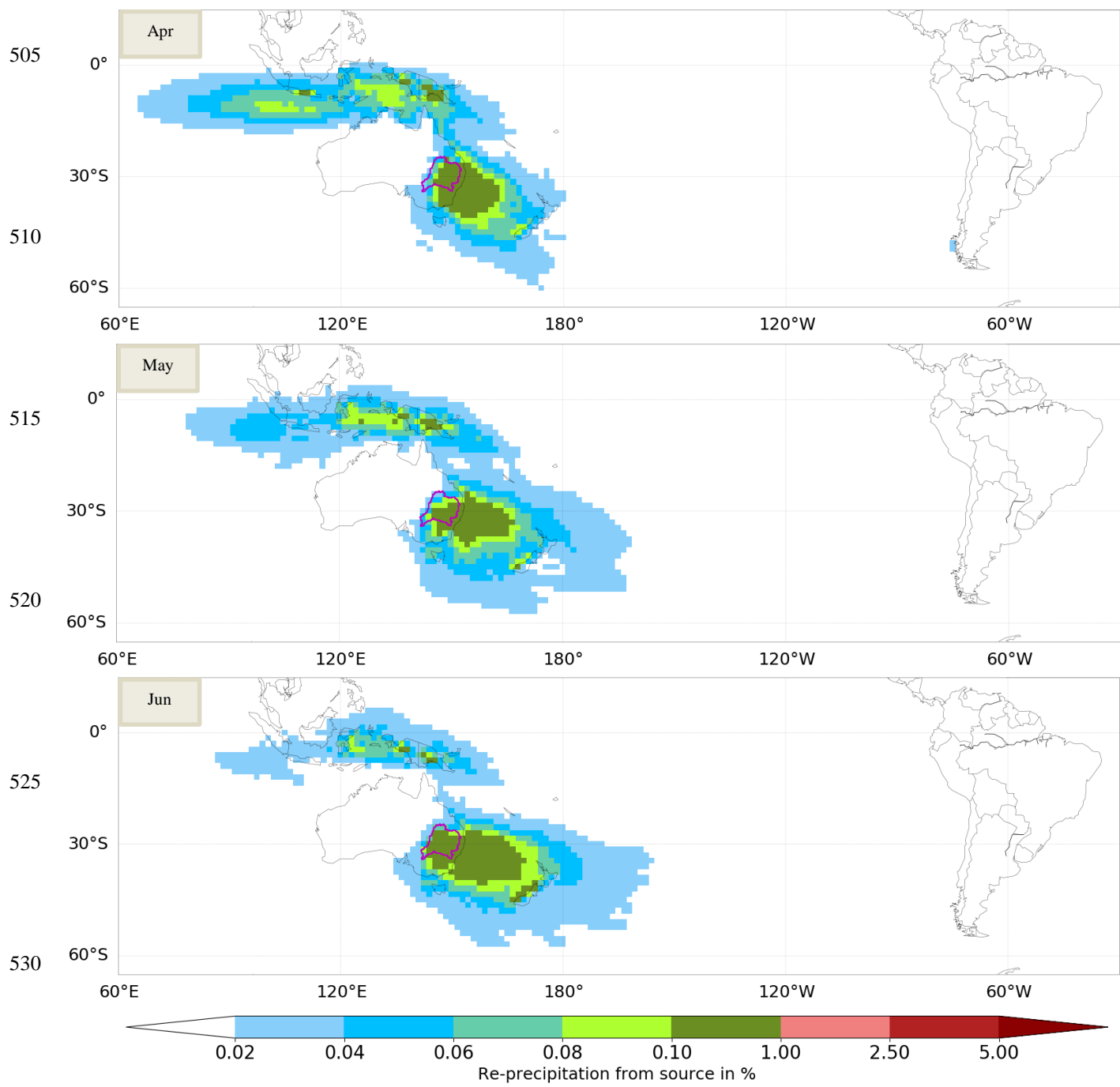


Figure S34 Monthly evaporation sheds (Apr = April, May, Jun = June) for the basin with the ID 2245569 (part of the Murray-Darling basin), E_{input} : 30.0 mm/month (Apr) / 21.6 mm/month (May) / 21.9 mm/month (Jun), Unassigned : 0.5 % (Apr) / 0.5 % (May) / 0.5 % (Jun), Colored area covers 59.9 % (Apr) / 61.4 % (May) / 60.8 % (Jun) of the assigned water

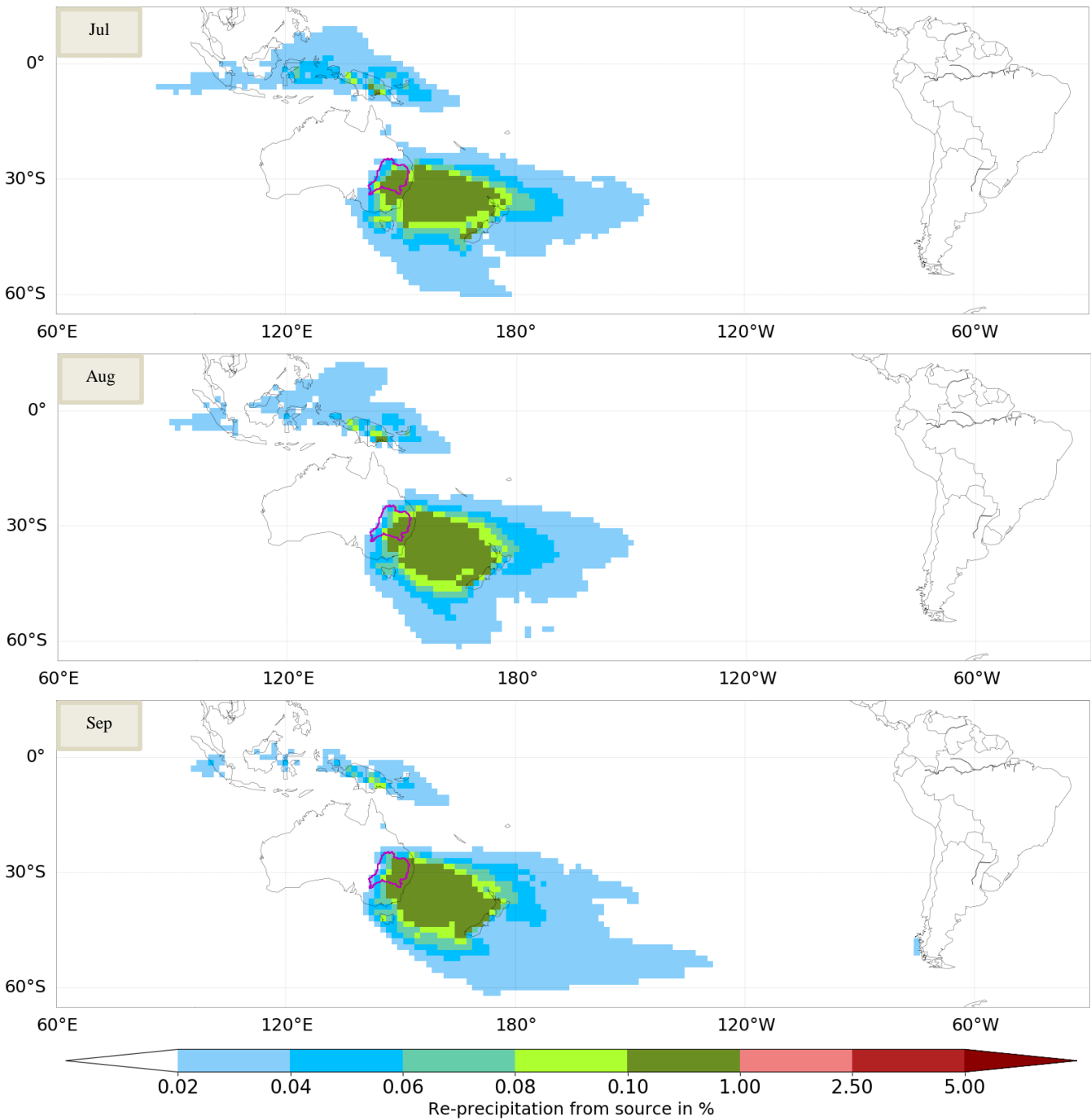


Figure S35 Monthly evaporationsheds (Jul = July, Aug = August, Sep = September) for the basin with the ID 2245569 (part of the Murray-Darling basin), E_{input} : 22.0 mm/month (Jul) / 25.6 mm/month (Aug) / 36.6 mm/month (Sep), Unassigned : 0.5 % (Jul) / 0.5 % (Aug) / 0.6 % (Sep), Colored area covers 60.1 % (Jul) / 60.6 % (Aug) / 61.7 % (Sep) of the assigned water

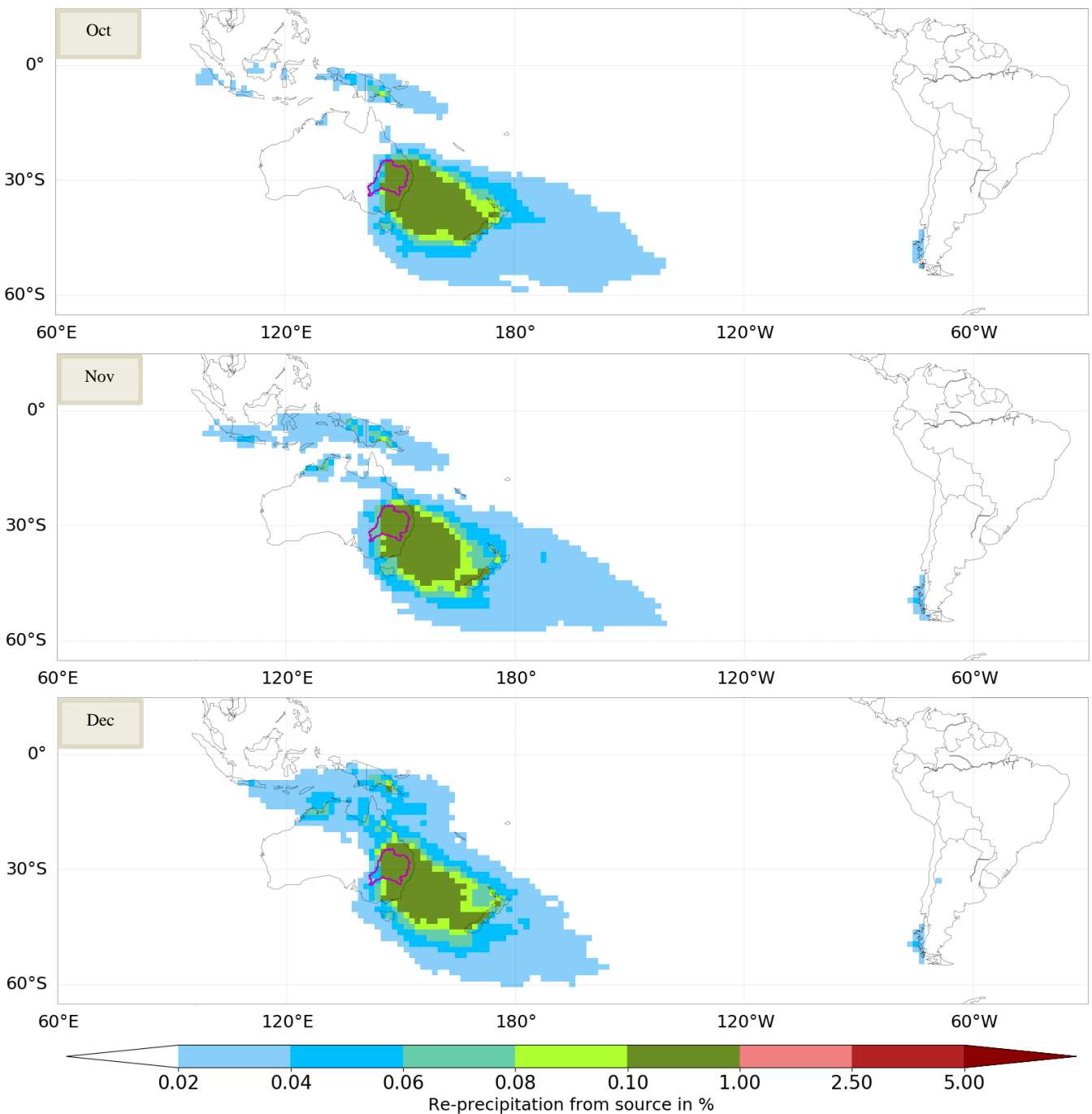


Figure S36 Monthly evaporationsheds (Oct = October, Nov = November, Dec = December) for the basin with the ID 2245569 (part of the Murray-Darling basin), E_{input} : 48.7 mm/month (Oct) / 57.2 mm/month (Nov) / 64.4 mm/month (Dec), Unassigned : 0.6 % (Oct) / 0.6 % (Nov) / 0.5 % (Dec), Colored area covers 59.3 % (Oct) / 62.0 % (Nov) / 64.0 % (Dec) of the assigned water

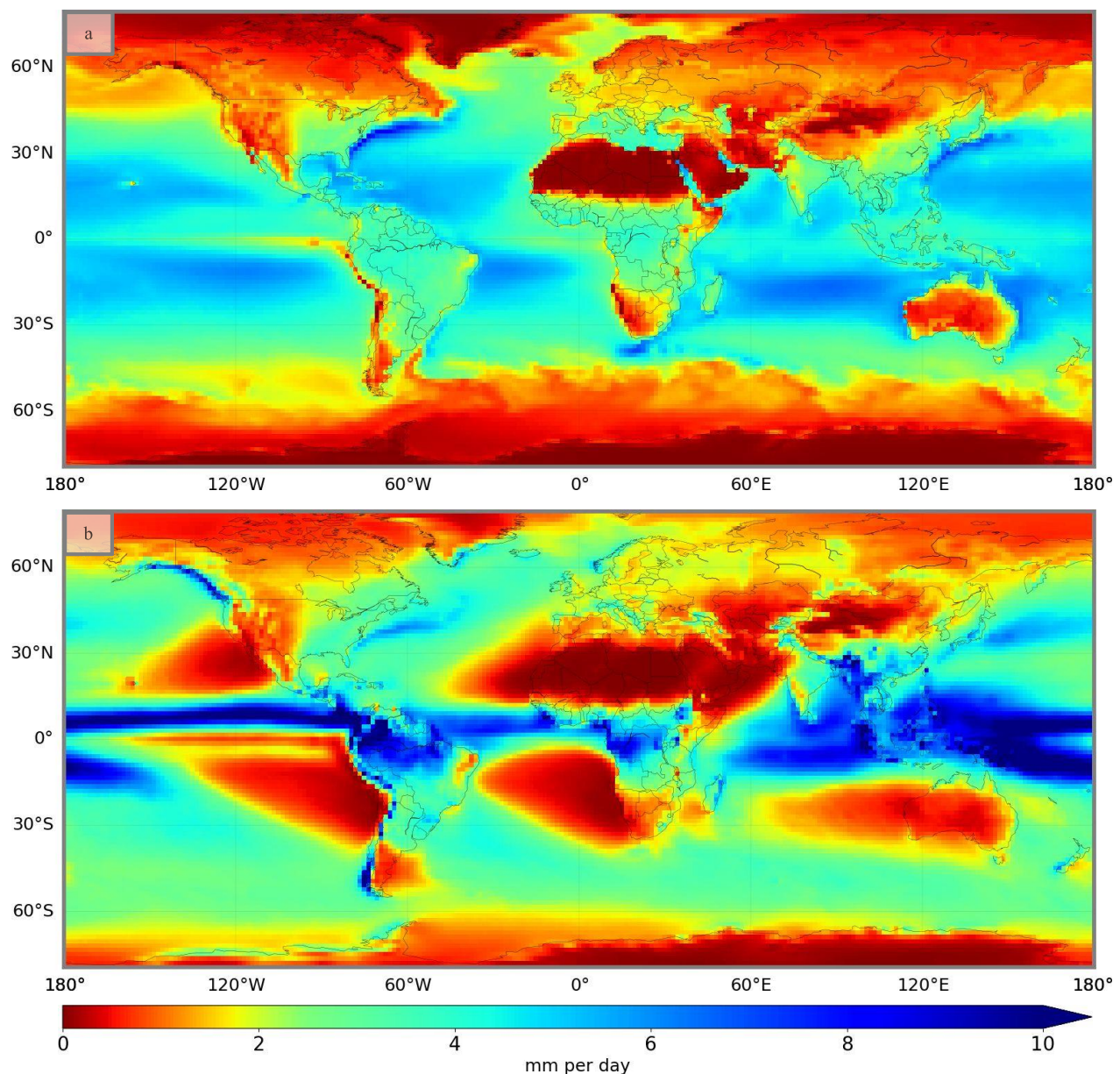


Figure S37 Average evaporation (a) and precipitation (b) in mm per day based on the ERA-Interim reanalysis (Berrisford et al., 2011; Dee et al., 2011); considered time period: 2001 to 2018

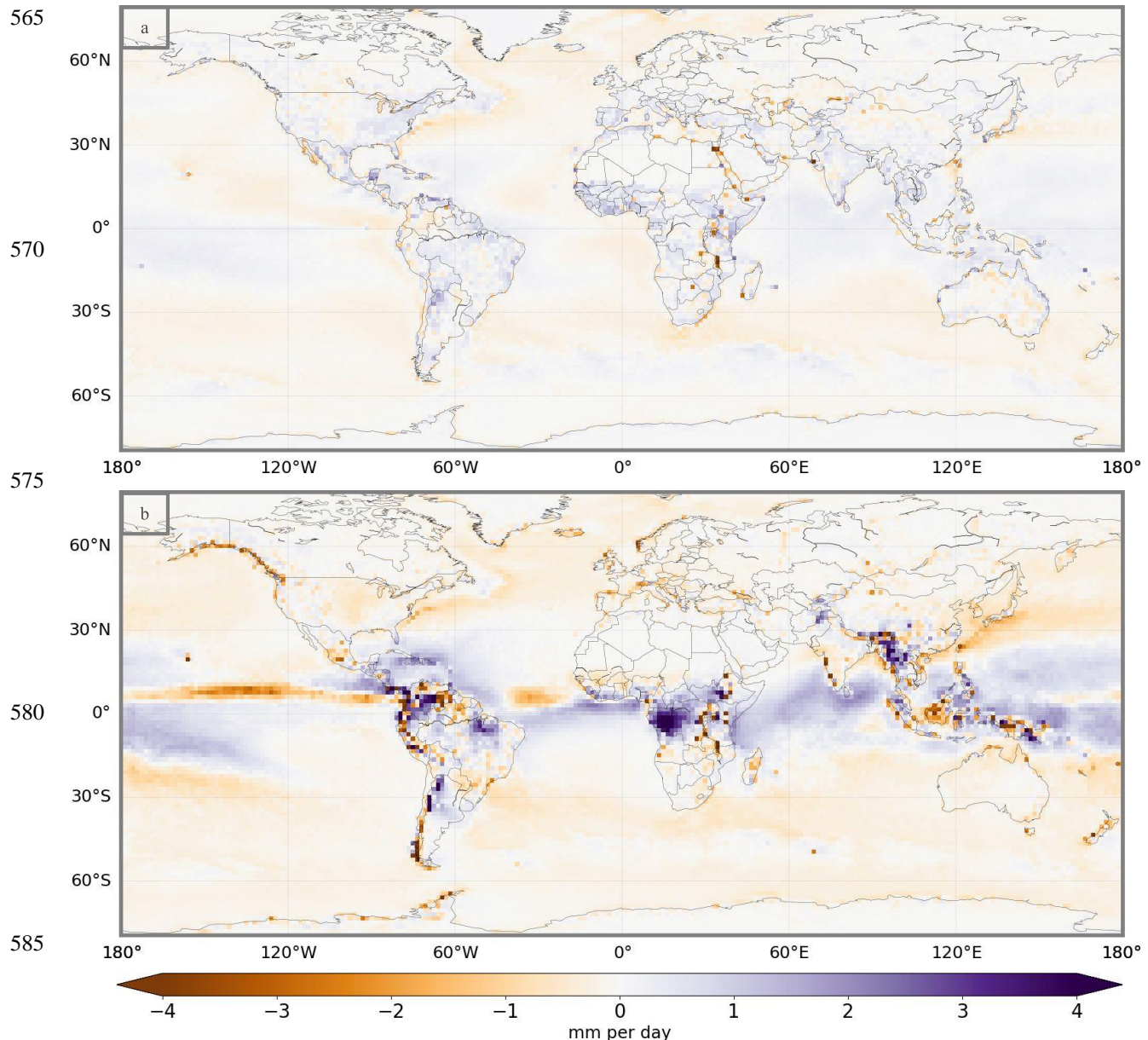


Figure S38 Differences between ERA-Interim (Berrisford et al., 2011; Dee et al., 2011) and ERA5 (Hersbach et al., 2020) regarding the average evaporation (a) and precipitation (b) in mm per day (ERA-Interim minus ERA5); considered time period: 2001 to 2018

590

Methodological details regarding the continental comparison of the average evaporation and precipitation between ERA-Interim (Berrisford et al., 2011; Dee et al., 2011), ERA5 (Hersbach et al., 2020) and the study by Rodell et al. 595 (2015)

Regarding the continental comparison of the average evaporation and precipitation between ERA-Interim (ERA-I), ERA5 and the study by Rodell et al. (2015) (Table 4 of the main article), we highlight the following two methodological elements:

- 600
- In order to enable a comparison of ERA-I and ERA5 to the continental results of the study by Rodell et al, values for the average evaporation and precipitation in ERA-I / ERA5 needed first to be aggregated to continental scales. We relied within this context on the country mask used for our article (Cun, 2016) and grouped within a second step our country results to continents. An overview on this grouping procedure can be gained through Table S1, which is presented below. Slight differences in continental delineations to the study of Rodell et al. (2015) might be possible 605 but are considered as negligible small.
 - We modified regarding the comparison the covered time horizon of the ERA-I and ERA5 data while excluding all data outside the first decade of the 21st century (2011 to 2018). This procedure led to a relatively high temporal overlap of the two data sources in comparison to Rodell et al (2015).

610

615

620

625

Table S1 Grouping of countries for the aggregation of the ERA-Interim and ERA5 data on evaporation and precipitation (Berrisford et al., 2011; Dee et al., 2011) to continental scales

North America
Anguilla, Antigua and Barbuda, Aruba, Bahamas, Barbados, Belize, Bermuda, Bonaire, British Virgin Islands, Canada, Cayman Islands, Clipperton Island, Costa Rica, Cuba, Curaçao, Dominica, Dominican Republic, El Salvador, Greenland, Grenada, Guadeloupe, Guatemala, Haiti, Honduras, Jamaica, Martinique, Mexico, Montserrat, Navassa Island, Nicaragua, Panama, Puerto Rico, Saint Barthélemy, Saint Kits and Nevis, Saint Lucia, Saint Martin, Saint Pierre and Miquelon, Saint Vincent and the Grenadines, Sint Maarten, Trinidad and Tobago, Turks and Caicas Islands, United States, Virgin Islands
South America
Argentina, Bolivia, Bouvet Island, Brazil, Chile, Colombia, Ecuador, Falkland Islands (Islas Malvinas), French Guiana, Guyana, Paraguay, Peru, South Georgia and the South Sandwich Islands, Suriname, Uruguay, Venezuela
Eurasia
Åland, Afghanistan, Albania, Andorra, Armenia, Austria, Azerbaijan, Bahrain, Brunei, Bangladesh, Belarus, Belgium, Bhutan, Bosnia and Herzegovina, British Indian Ocean Territory, Bulgaria, Burma, Cambodia, China, Christmas Island, Cocos (Keeling) Islands, Croatia, Cyprus, Czech Republic, Denmark, Estonia, Faroe Islands, Finland, France, Palestine, Georgia, Germany, Gibraltar, Greece, Guernsey, Hong Kong, Hungary, Iceland, India, Indonesia, Iran, Iraq, Ireland, Isle of Man, Israel, Italy, Japan, Jersey, Jordan, Kazakhstan, Kuwait, Kyrgyzstan, Laos, Latvia, Lebanon, Liechtenstein, Lithuania, Luxembourg, Macau, Macedonia, Malaysia, Maldives, Malta, Moldova, Monaco, Mongolia, Montenegro, Nepal, Netherlands, North Korea, Norway, Oman, Pakistan, Paracel Islands, Philippines, Poland, Portugal, Qatar, Romania, Russia, San Marino, Saudi Arabia, Serbia, Singapore, Slovakia, Slovenia, South Korea, Spain, Spratly Islands, Sri Lanka, Svalbard and Jan Mayen, Sweden, Switzerland, Syria, Taiwan, Tajikistan, Thailand, Timor-Leste, Turkey, Turkmenistan, Ukraine, United Arab Emirates, United Kingdom, Uzbekistan, Vatican City, Vietnam, Yemen
Africa
Algeria, Angola, Benin, Botswana, Burkina Faso, Burundi, Cameroon, Cape Verde, Central African Republic, Chad, Comoros, Congo, DR Congo, Côte d'Ivoire, Djibouti, Egypt, Equatorial Guinea, Eritrea, Ethiopia, Europa Island, French Southern and Antarctic Lands, Gabon, Gambia, Ghana, Glorioso Islands, Guinea, Guinea-Bissau, Heard Island and McDonald Islands, Juan De Nova Island, Kenya, Lesotho, Liberia, Libya, Madagascar, Malawi, Mali, Mauritania, Mauritius, Mayotte, Morocco, Mozambique, Namibia, Niger, Nigeria, Reunion, Rwanda, Saint Helena, Sao Tome and Principe, Senegal, Seychelles, Sierra Leone, Somalia, South Africa, Sudan / South Sudan, Swaziland, Tanzania, Togo, Tromelin Island, Tunisia, Uganda, Western Sahara, Zambia, Zimbabwe
Australia
Oceania
American Samoa, Ashmore and Cartier Islands, Baker Island, Cook Islands, Coral Sea Islands, Federated States of Micronesia, Fiji, French Polynesia, Guam, Howland Island, Jarvis Island, Kingman Reef, Kiribati, Marshall Islands, Nauru, New Caledonia, New Zealand, Niue, Norfolk Island, Northern Mariana Islands, Palau, Vanuatu, Palmyra Atoll, Papua New Guinea, Pitcairn Islands, Samoa, Solomon Islands, Tokelau, Tonga, Tuvalu, Wake Island, Wallis and Futuna
Unassigned regions
Johnston Atoll, Midway Islands

Table S2 Terrestrial evaporative source (TES – unit: %) as well as the country internal evaporative source (CIES – unit: %) for precipitation in different countries – Comparison of the results between the 3D QIBT model (fed with NCEP-DOE AMIP-II data (Kanamitsu et al., 2002) for wind and evaporation and CMAP data (Xie and Arkin, 1997) for precipitation) applied by Dirmeyer et al. (2009) and the WAM-2layers model (fed with ERA-Interim data (Berrisford et al., 2011; Dee et al., 2011))

	TES in %		CIES in %	
	3D QIBT	WAM-2layers	3D QIBT	WAM-2 layers
North America				
Belize	19.5	15.5	0.5	1.4
Canada	69.7	38.6	54.8	17.4
Costa Rica	34.3	19.3	2.4	1.6
El Salvador	30.0	22.9	1.4	1.7
Guatemala	25.3	22.8	4.0	4.6
Honduras	24.7	18.9	4.2	4.6
Mexico	39.7	28.6	28.4	16.2
Nicaragua	25.9	16.7	5.1	2.7
Panama	42.6	25.1	5.4	2.1
United States	52.5	30.2	43.2	18.3
South America				
Argentina	59.5	50.6	27.9	19.0
Bolivia	82.7	59.4	24.2	16.0
Brazil	56.7	36.7	46.3	28.9
Chile	8.1	4.3	5.4	1.4
Colombia	49.9	37.1	10.9	11.6
Ecuador	62.7	38.5	4.9	7.6
French Guiana	14.5	12.0	2.6	2.3
Guyana	19.1	16.4	3.2	3.2
Paraguay	90.0	61.9	13.0	6.5
Peru	71.8	49.2	25.9	16.5
Suriname	18.2	14.8	2.8	3.0
Uruguay	75.1	55.3	8.1	2.8
Venezuela	29.4	27.0	9.1	9.8
Europe				
Albania	31.9	31.3	2.6	1.3
Armenia	60.8	59.3	3.9	3.2
Austria	54.4	41.9	6.7	2.9
Azerbaijan	59.2	51.6	6.5	4.0
Belarus	67.2	42.1	12.3	3.5

	TES in %		CIES in %	
	3D QIBT	WAM-2layers	3D QIBT	WAM-2 layers
Belgium	26.7	25	2.9	1.0
Bosnia and Herzegovina	42.7	33.8	6.6	1.9
Bulgaria	53.3	42.2	7.2	4.2
Croatia	47.3	33.7	5.1	1.7
Czech Republic	54.5	38.6	5.5	2.5
Denmark	27.1	25.1	2.9	1.1
Estonia	52.8	33.5	4.7	1.3
Finland	58.7	34.8	19.2	3.3
France	26.0	24.7	12.6	5.5
Georgia	60.9	53.7	7.3	4.0
Germany	39.2	31.2	11.9	4.3
Greece	30.2	31.6	8.2	3.7
Hungary	60.8	40.1	7.1	2.7
Iceland	16.8	16.7	8.8	1.0
Ireland	11.1	16.8	5.3	1.3
Italy	39.8	33.6	14.2	5.6
Latvia	54.0	35.6	4.8	1.6
Lithuania	54.4	37.3	4.9	1.7
Luxembourg	28.8	26.4	0.4	0.2
Macedonia	37.6	38.8	1.4	1.6
Moldova	70.1	45.7	3.4	1.5
Netherlands	25.0	24.1	3.1	1.1
Norway	26.0	23.8	10.9	2.3
Poland	56.1	38.5	14.0	4.1
Portugal	9.9	12.4	3.9	1.6
Romania	66.1	46.5	15.3	6.3
Russia	83.2	53.9	64.7	27.8
Slovakia	63.2	42.2	5.6	1.4
Slovenia	53.8	40.5	3.3	1.5
Spain	19.3	21.0	12.6	6.3
Sweden	42.8	31.2	18.7	4.0
Switzerland	42.5	36.5	6.4	2.3
Ukraine	69.0	43.5	19.0	6.6
United Kingdom	14.9	19.1	6.4	2.2

	TES in %		CIES in %	
	3D QIBT	WAM-2layers	3D QIBT	WAM-2 layers
Africa				
Algeria	24.6	31.6	8.3	5.0
Angola	81.3	58.1	23.6	20.9
Benin	66.0	57.2	5.2	4.9
Botswana	82.9	56.6	17.9	10.9
Burkina Faso	73.5	63.0	10.3	7.9
Burundi	55.8	40.8	1.9	3.2
Cameroon	78.6	64.0	11.4	11.7
Central African Republic	82.0	62.1	11.8	12.9
Chad	68.0	68.0	15.7	12.4
Congo	80.9	58.8	10.6	9.5
Cote d'Ivoire	61.2	47.6	9.1	9.4
Djibouti	47.8	37.5	1.3	0.9
Egypt	17.6	23.4	2.8	2.7
Equatorial Guinea	73.3	60.8	1.2	4.2
Eritrea	51.9	48.0	4.0	4.1
Ethiopia	56.4	44.2	25.6	15.9
Gabon	71.2	59.4	9.9	10.0
Gambia	60.3	53.6	0.7	0.8
Ghana	62.5	48.0	8.1	7.8
Guinea	64.7	58.5	7.3	7.5
Guinea-Bissau	56.5	51.7	3.0	2.3
Kenya	34.8	22.9	11.9	9.2
Lesotho	68.9	48.7	3.9	2.7
Liberia	50.5	44.1	3.5	4.3
Libya	19.8	28.5	5.0	2.3
Madagascar	27.4	18.1	20.5	11.6
Malawi	60.0	37.1	6.6	3.5
Mali	31.9	66.8	17.4	10.7
Mauritania	58.7	62.8	8.6	4.2
Morocco	12.7	21.8	7.7	5.2
Mozambique	49.5	29.3	20.2	11.5

	TES in %		CIES in %	
	3D QIBT	WAM-2layers	3D QIBT	WAM-2 layers
Namibia	84.2	60.7	20.6	12.6
Niger	60.0	72.0	17.8	8.2
Nigeria	66.2	58.8	18.8	14.4
Rwanda	57.0	40.9	1.4	2.6
Senegal	64.2	58.4	6.5	6.0
Sierra Leone	53.6	51.2	3.9	4.1
Somalia	22.2	14.5	7.4	6.7
South Africa	61.6	43.3	23.1	14.4
Sudan + South Sudan	70.9	54.5	20.1	17.4
Swaziland	62.0	43.3	1.7	1.7
Tanzania	41.6	31.5	17.4	14.1
Togo	53.1	53.5	1.9	3.0
Tunisia	24.9	29.2	3.8	2.8
Uganda	60.6	36.7	10.3	9.3
Western Sahara	18.8	29.0	1.5	0.9
DR Congo	75.2	52.0	28.5	25.1
Zambia	73.2	51.3	19.0	13.9
Zimbabwe	70.5	45.5	16.2	10.3
Western Asia				
Afghanistan	51.3	44.7	11.1	8.5
Bangladesh	57.8	34.7	4.7	3.0
Bhutan	84.0	48.0	3.7	2.0
India	60.3	36.6	36.4	18.1
Iran	41.5	35.8	11.2	7.0
Iraq	32.3	31.9	4.9	3.7
Israel	13.3	21.8	0.8	0.8
Jordan	16.1	26.7	1.5	0.9
Kazakhstan	76.2	50.8	21.5	10.7
Kyrgyzstan	73.6	60.9	10.6	8.4
Lebanon	13.7	22.7	1.5	0.5
Nepal	85.5	48.6	12.5	5.5
Oman	37.6	20.9	2.0	1.6

	TES in %		CIES in %	
	3D QIBT	WAM-2layers	3D QIBT	WAM-2 layers
Pakistan	67.8	50.8	15.8	12.9
Qatar	45.5	24.0	0.4	0.3
Saudi Arabia	46.3	30.2	8.2	6.4
Sri Lanka	16.7	13.1	5.4	2.3
Syria	23.1	28.8	4.4	2.7
Tajikistan	63.1	53.9	6.9	6.3
Turkey	40.9	36.3	22.3	9.8
Turkmenistan	50.8	39.0	4.3	3.3
United Arab Emirates	47.2	23.5	1.7	1.5
Uzbekistan	59.2	42.7	5.3	4.2
Yemen	50.4	39.1	5.9	5.6
Eastern Asia & Oceania				
Australia	38.6	22.9	37.9	20.7
Burma	49.3	29.3	12.6	6.7
Cambodia	23.0	19.0	5.8	5.9
China	74.8	56.2	41.4	25.9
Indonesia	28.2	18.6	22.3	12.2
Japan	36.6	26.6	10.1	3.3
Laos	43.7	30.0	6.6	4.1
Malaysia	30.5	18.3	10.5	6.3
Mongolia	95.7	80.3	30.8	12.4
New Zealand	9.9	8.8	6.7	2.2
North Korea	67.9	48.6	7.4	2.4
Papua New Guinea	29.3	12.2	19.1	7.2
Philippines	11.6	9.3	6.3	3.4
South Korea	47.2	32.4	5.5	1.6
Thailand	30.3	22.4	9.3	6.8
Vietnam	33.6	25.7	6.7	4.1

Table S3 Top 10 sources of precipitation for the country Brazil – Comparison between results from the 3D QIBT model (fed with NCEP-DOE AMIP-II data (Kanamitsu et al., 2002) for wind and evaporation and CMAP data (Xie and Arkin, 1997) for precipitation) and the WAM-2layers model (fed with ERA-Interim data (Berrisford et al., 2011; Dee et al., 2011)) – Sources appearing in both lists are displayed in bold font; UA = Unassigned fractions due to system boundary losses

Rank	Top 10 sources of precipitation for Brazil in %			
	3D QIBT		WAM-2layers	
1	Brazil	46.3	Sea	63.3
2	Sea	43.3	Brazil	28.9
3	Bolivia	2.4	Bolivia	1.2
4	Peru	1.3	Peru	0.6
5	Argentina	1.2	Argentina	0.6
6	Paraguay	0.9	Angola	0.4
7	Nigeria	0.6	Paraguay	0.4
8	Côte d'Ivoire	0.5	Venezuela	0.3
9	Ghana	0.4	Guyana	0.3
10	Other land	2.9	Other land + UA	4.0

Table S4 Top 10 sources of precipitation for the country Egypt – Comparison between results from the 3D QIBT model (fed with NCEP-DOE AMIP-II data (Kanamitsu et al., 2002) for wind and evaporation and CMAP data (Xie and Arkin, 1997) for precipitation) and the WAM-2layers model (fed with ERA-Interim data (Berrisford et al., 2011; Dee et al., 2011)) – Sources appearing in both lists are displayed in bold font; UA = Unassigned fractions due to system boundary losses

Rank	Top 10 sources of precipitation for Egypt in %			
	3D QIBT		WAM-2layers	
1	Sea	82.4	Sea	76.6
2	Libya	3.3	Egypt	2.7
3	Egypt	2.8	Turkey	1.9
4	Algeria	1.4	Greece	1.2
5	Greece	1.0	Libya	1.1
6	Spain	1.0	Sudan / South Sudan	0.9
7	Sudan / South Sudan	0.7	Algeria	0.9
8	Morocco	0.6	Nigeria	0.8
9	Turkey	0.6	United States	0.8
10	Other land	6.0	Other land + UA	13.1

650 **Table S5 Top 10 sources of precipitation for the country Laos – Comparison between results from the 3D QIBT model (fed with NCEP-DOE AMIP-II data (Kanamitsu et al., 2002) for wind and evaporation and CMAP data (Xie and Arkin, 1997) for precipitation) and the WAM-2layers model (fed with ERA-Interim data (Berrisford et al., 2011; Dee et al., 2011)) – Sources appearing in both lists are displayed in bold font; UA = Unassigned fractions due to system boundary losses**

Rank	Top 10 sources of precipitation for Laos in %			
	3D QIBT		WAM-2layers	
1	Sea	56.3	Sea	70.0
2	Thailand	9.4	Thailand	6.4
3	Burma	6.9	Laos	4.1
4	Laos	6.6	India	3.9
5	India	6.2	Burma	3.6
6	China	5.2	China	3.4
7	Vietnam	4.0	Vietnam	1.9
8	Cambodia	2.2	Cambodia	1.3
9	Pakistan	0.4	Indonesia	0.4
10	Other land	2.9	Other land + UA	5.0

655

660

665

670

References of the supplement

- Berrisford, P., Dee, D. P., Poli, P., Brugge, R., Fielding, K., Fuentes, M., Källberg, P., Kobayashi, S., Uppala, S. and Simmons, A.: The ERA-Interim archive Version 2.0. ERA Report Series 1. [online] Available from: <http://www.ecmwf.int/en/elibrary/8174-era-interim-archive-version-20>, 2011.
- 675 Cun, J. L.: Global country boundaries, [online] Available from: <https://www.arcgis.com/home/item.html?id=2ca75003ef9d477fb22db19832c9554f> (Accessed 27 September 2019), 2016.
- Dee, D. P., Uppala, S. M., Simmons, A. J., Berrisford, P., Poli, P., Kobayashi, S., Andrae, U., Balmaseda, M. A., Balsamo, G., Bauer, P., Bechtold, P., Beljaars, A. C. M., van de Berg, L., Bidlot, J., Bormann, N., Delsol, C., Dragani, R., Fuentes, M., Geer, A. J., Haimberger, L., Healy, S. B., Hersbach, H., Hólm, E. V., Isaksen, L., Källberg, P., Köhler, M., Matricardi, M., 680 McNally, A. P., Monge-Sanz, B. M., Morcrette, J. J., Park, B. K., Peubey, C., de Rosnay, P., Tavolato, C., Thépaut, J. N. and Vitart, F.: The ERA-Interim reanalysis: Configuration and performance of the data assimilation system, *Q. J. R. Meteorol. Soc.*, 137(656), 553–597, doi:10.1002/qj.828, 2011.
- Dirmeyer, P. A., Brubaker, K. L. and DelSole, T.: Import and export of atmospheric water vapor between nations, *J. Hydrol.*, 365(1–2), 11–22, doi:10.1016/j.jhydrol.2008.11.016, 2009.
- 685 Hersbach, H., Bell, B., Berrisford, P., Hirahara, S., Horányi, A., Muñoz-Sabater, J., Nicolas, J., Peubey, C., Radu, R., Schepers, D., Simmons, A., Soci, C., Abdalla, S., Abellán, X., Balsamo, G., Bechtold, P., Biavati, G., Bidlot, J., Bonavita, M., de Chiara, G., Dahlgren, P., Dee, D., Diamantakis, M., Dragani, R., Flemming, J., Forbes, R., Fuentes, M., Geer, A., Haimberger, L., Healy, S., Hogan, R. J., Hólm, E., Janisková, M., Keeley, S., Laloyaux, P., Lopez, P., Lupu, C., Radnoti, G., de Rosnay, P., Rozum, I., Vamborg, F., Villaume, S. and Thépaut, J.-N.: The ERA5 Global Reanalysis, *R. Meteorol. Soc., Preprint*, 690 doi:10.1002/qj.3803., 2020.
- Kanamitsu, M., Ebisuzaki, W., Woollen, J., Yang, S. K., Hnilo, J. J., Fiorino, M. and Potter, G. L.: NCEP-DOE AMIP-II reanalysis (R-2), *Bull. Am. Meteorol. Soc.*, doi:10.1175/bams-83-11-1631(2002)083<1631:nar>2.3.co;2, 2002.
- Link, A., Van der Ent, R., Berger, M., Eisner, S. and Finkbeiner, M.: The fate of land evaporation - A global dataset, PANGAEA, , doi:<https://doi.org/10.1594/PANGAEA.908705>, 2019a.
- 695 Link, A., Van der Ent, R., Berger, M., Eisner, S. and Finkbeiner, M.: Tool for Visualizing the Fate of Land Evaporation, [online] Available from: <https://wf-tools.see.tu-berlin.de/wf-tools/evaporationshed/#/> (Accessed 16 December 2019), 2019b.
- Rodell, M., Beaudoin, H. K., L'Ecuyer, T. S., Olson, W. S., Famiglietti, J. S., Houser, P. R., Adler, R., Bosilovich, M. G., Clayson, C. A., Chambers, D., Clark, E., Fetzer, E. J., Gao, X., Gu, G., Hilburn, K., Huffman, G. J., Lettenmaier, D. P., Liu, W. T., Robertson, F. R., Schlosser, C. A., Sheffield, J. and Wood, E. F.: The observed state of the water cycle in the early 700 twenty-first century, *J. Clim.*, 28(21), 8289–8318, doi:10.1175/JCLI-D-14-00555.1, 2015.
- Van der Ent, R. J.: A new view on the hydrological cycle over continents, Ph.D. thesis, Delft University of Technology, Delft, 96 pp., 2014.
- Xie, P. and Arkin, P. A.: Global Precipitation: A 17-Year Monthly Analysis Based on Gauge Observations, Satellite Estimates,

and Numerical Model Outputs, Bull. Am. Meteorol. Soc., doi:10.1175/1520-0477(1997)078<2539:GPAYMA>2.0.CO;2,

705 1997.